UCRL-11417

University of California

Ernest O. Lawrence Radiation Laboratory

TWO-WEEK LOAN COPY

This is a Library Circulating Copy which may be borrowed for two weeks. For a personal retention copy, call Tech. Info. Division, Ext. 5545

LITHIUM ALLOYING AND DISLOCATION MECHANISMS FOR PRISMATIC SLIP IN MAGNESIUM

Berkeley, California

DISCLAIMER

This document was prepared as an account of work sponsored by the United States Government. While this document is believed to contain correct information, neither the United States Government nor any agency thereof, nor the Regents of the University of California, nor any of their employees, makes any warranty, express or implied, or assumes any legal responsibility for the accuracy, completeness, or usefulness of any information, apparatus, product, or process disclosed, or represents that its use would not infringe privately owned rights. Reference herein to any specific commercial product, process, or service by its trade name, trademark, manufacturer, or otherwise, does not necessarily constitute or imply its endorsement, recommendation, or favoring by the United States Government or any agency thereof, or the Regents of the University of California. The views and opinions of authors expressed herein do not necessarily state or reflect those of the United States Government or any agency thereof or the Regents of the University of California.

Research and Development

UCRL-11417

UNIVERSITY OF CALIFORNIA
Lawrence Radiation Laboratory
Berkeley, California

AEC Contract No. W-7405-eng-48

LITHIUM ALLOYING AND DISLOCATION MECHANISMS FOR PRISMATIC SLIP IN MAGNESIUM

Aziz Ahmadieh

(Ph. D. Thesis)

May 18, 1964

Printed in USA. Price $1.50. Available from the
Office of Technical Services
U. S. Department of Commerce
Washington 25, D.C.

LITHIUM ALLOYING AND DISLOCATION MECHANISMS FOR PRISMATIC SLIP IN MAGNESIUM

Contents

Abstract v

I. Introduction 1

II. Experimental Technique 3

III. Experimental Results 7

IV. Discussion 20

A. Effect of Temperature and Strain-Rate on Flow Stress . 30

B. Activation Energy for Nucleation of Pairs of Kinks . . . 34

C. Activation Volume 35

D. Evaluation of Line Tension of Dislocation Situated at the Peierls Valley 36

E. Effect of Temperature and Strain-Rate on Critical Shear Stress. 39

F. Activation Energy for Nucleation of Pairs of Kinks . . . 39

G. Activation Volume 42

H. Evaluation of Line Tension of Dislocation Situated at the Peierls Valley 42

I. Effect of Temperature on the Yield Strength 45

J. Effect of Change in Strain Rate on the Stress 47

V. Conclusions 53

Acknowledgments 55

References 56

LITHIUM ALLOYING AND DISLOCATION MECHANISMS FOR PRISMATIC SLIP IN MAGNESIUM

Aziz Ahmadieh

Department of Mineral Technology and
Inorganic Materials Research Division, Lawrence Radiation Laboratory
University of California, Berkeley, California

May 18, 1964

ABSTRACT

An investigation was made to determine the role of lithium alloying on the dislocation rate controlling mechanisms of magnesium oriented for $(10\bar{1}0)$ $[1\bar{2}10]$ prismatic slip using three alloys, namely, 12.5, 10.8 and 6.8 at.% Li-Mg. Whereas prismatic slip was preceeded by twinning and fracturing at temperatures below 450°K in pure magnesium, the alloy containing 6.8 at.% Li was ductile at temperatures as low as 200°K. The higher Li alloys showed more than 20% shear strain at 4.2°K and finally fractured on the prismatic planes upon initiation of duplex slip. The data revealed that the alloys have a critical resolved shear stress lower than that of pure Mg showing that the Li-Mg alloys provide an exception to one of the usual trends of alloying, namely, that solid solutions are stronger than the pure parent metals. This decrease in the flow stress is enhanced by increasing in the lithium content.

Whereas the flow stress increased only slightly with decrease in test temperature below 400 and 370°K for the 12.5 and 10.8 at.% Li alloys respectively, a rapid increase in the flow stress was obtained at temperatures below room temperature in all three alloys. The effect of both temperature and strain rate on the flow stress in the low temperature range could be completely rationalized in terms of the

Peierls mechanism when the deformation is controlled by the rate of nucleation of pairs of kinks.

Neither the Peierls mechanism nor the dislocation intersection mechanism can account for the data obtained from the 6.8 at.% Li alloy at high temperatures. However, the data are in excellent agreement with the dictates of Friedel's theory for cross-slip to the prismatic plane.

The separation of the dislocation partials on the basal plane and their constriction energy are lower in Li-Mg alloys than in pure Mg suggesting the increase of stacking fault energy with the addition of lithium.

I. INTRODUCTION

Investigations[1,2] on the deformation of polycrystalline aggregates of high purity Mg at low temperatures have shown that in addition to basal slip, small amounts of localized prismatic slip are induced to take place in regions of high stress concentration adjacent to grain boundaries and in the vicinity of the junction of three grains. This suggested that the critical resolved shear stress for prismatic slip is somewhat greater than that for basal slip in high purity Mg. This was later confirmed by a comparison of experimental data obtained on single crystals by Flynn[3] and Shelly and Nash.[4]

Further investigation on the mechanisms of plastic deformation of single and polycrystalline Mg resulted in the identification of the following mechanisms; $\{0001\}$,[5,2,6] $\{10\bar{1}0\}$,[2] $\{10\bar{1}1\}$[5,6,7] slip plus $\{10\bar{1}2\}$[5] and $\{30\bar{3}4\}$[8,9] twinning. The Burgers vector for active slip on both the basal and prismatic planes of Mg is, $b = a/3 \langle 1\bar{2}10 \rangle$.

For basal slip, recent investigations[10,11,4] have clearly shown that the strain-rate controlling mechanism at low temperatures is the thermally activated intersection of the glide dislocations with dislocations threading the basal plane.

Prismatic slip was studied in greater detail in single crystals of pure Mg[3] and it was revealed that below 450°K twinning and fracturing preceeded prismatic slip whereas above 450°K extensive slip was obtained. Over the latter region, the rate of prismatic slip was found to be in good agreement with the theory of thermally activated cross-slipping of screw dislocations extended in the basal plane.

When the deformation and fracture of polycrystalline Mg at low temperatures[2] was investigated, it was found that brittle fracture invariably occurred at subatmospheric temperatures. Hauser, Landon and Dorn[12] found that the addition of Li in the alpha solid solution range lowered the ductile to brittle transition temperatures to below 4°K. Their investigation also revealed that both the basal and prismatic slip mechanisms were operative, but the prismatic slip was more prevalent suggesting that it operated as an additional facile mechanism of deformation rather than as a localized stress relief mechanism at points of high stress concentration. The reason for this relatively easier operation of prismatic slip and the resulting increase in ductility was not determined.

In order to evaluate the process by which addition of a Li seemed to enhance the ease of prismatic slip, the rate controlling mechanisms of prismatic and basal slip in Mg-Li single crystals alloys were investigated. In a previous investigation of the effect of Li alloying on the basal slip,[13] complications arising from twinning, kinking, and accomodation bending in areas adjacent to subgrain boundaries prevented unquestionable identification of the actual rate controlling mechanism. However, the data revealed that the alloy containing 12.5 at.% Li has a critical resolved basal shear stress at least ten times that of pure Mg and that the critical resolved shear stress was temperature dependent below 250°K and relatively temperature insensitive above this point suggesting that as in pure Mg, basal slip may be controlled by the intersection mechanism.

The purpose of this investigation was to determine the rate controlling mechanism of prismatic slip in single crystals of an alpha solid solution of Mg containing various percent Li.

II. EXPERIMENTAL TECHNIQUE

One inch round extruded rods of Mg-Li alloys of the following analyses were used for this investigation.* Table I

Single crystal spheres of pure Mg were grown by directional solidification in a graphite mold under an argon atmosphere using a modified Bridgman technique. The spheres were oriented by Laue back-reflection technique and used to seed 3/8" diam cylindrical crystals of pure Mg. All seeds were oriented so that the angle (χ) between the tensile axis and the prismatic plane $(10\bar{1}0)$ was 45° and the angle (λ) between the tensile axis and the slip direction $\langle 1\bar{2}10 \rangle$ was also 45°. The oriented Mg crystals were then cut by an acid saw into 1" lengths to be used as seeds for the Mg-Li crystals.

The extruded alloys rods were machined into crystal blanks of the following dimensions

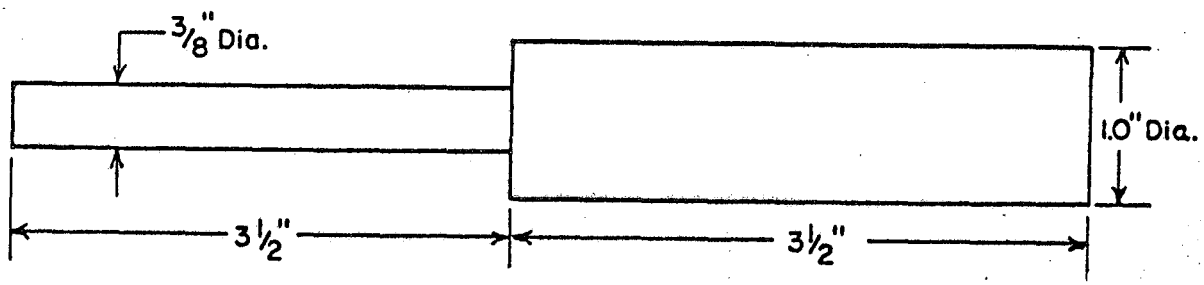

Fig. 1 Configuration of Mg-Li Single Crystal Blanks

The alloy crystals were grown under an argon atmosphere in a split (AISI 1020) steel mold having a 4" solid steel heat sink below

*Alloys and Analysis were furnished by courtesy of Dow Chemical Co.

TABLE I

Chemical Composition in Weight Percent

Alloy No.	Al	Ca	Cu	Fe	Un	Ni	Si	Zn	Mg	Li
1	<0.03	0.147	<0.001	0.007	<0.01	<0.001	<0.01	<0.02	Bal.	6.01
2	"	"	"	"	"	"	"	"	Bal.	5.02
3	"	"	"	"	"	"	"	"	Bal.	3.01

the seed to produce a steep temperature gradient across the interface. The solid to liquid interface traversed the length of the 3/8" section at a rate of 1/4" per hour. After the alloy had solidified, it was carefully removed from the mold. The 3/8" diam test section of the single crystal was acid cut to a length of 3-1/2" by removing the seed and the 1" diam reservoir section. By using a 1" reservoir section on the crystal blank, the crystal itself is then only 1/8 of the total weight of alloy. Thus, when the crystal proper was solidified, only 1/8 of the total melt has been removed and the composition gradient over the gage length is kept to less than 0.5 at.%. The initial 4 crystals of each alloy were analysed by flame photometry to determine the composition gradient. Table II shows the composition analyses of the 3 alloys and the assumed average.

The crystals were annealed in argon for 15 min at 773°K to remove any cold work imposed by their removal from the mold. The exact orientation was then determined by the Laue back-reflection technique.

By masking all but a 1" section in the center of the crystal with electroplaters tape, a reduced gage section of about 0.2" diam by 1" long was obtained by acid milling in a 15% solution of HCl. The rate of attack of the acid was very uniform, retaining the cylindrical shape of the original crystal, and rounded fillets were produced on the ends of the test section. The use of a 1" test section permitted the grips to be attached 1/2" from the fillets so that grip effect would be minimized. Thermocouples were attached to each grip in such a manner that the temperature differential recorded during all tests was 1°K between the ends of the gage length.

The crystals were tested in tension on an Instron TTCL machine operated at the strain rates of 0.333×10^{-4}, 3.33×10^{-4} and

TABLE II

Composition Gradients in the Single Crystals

Alloy No.	Crystal No.	at. % Lithium in Gage Section Lower End	Upper End
1	1	12.5	12.0
	2	12.3	12.5
	3	12.75	12.5
	4	12.5	12.4
		Average 12.5 at. % Li ± 0.3	
2	1	10.83	10.90
	2	10.75	10.80
	3	10.88	10.72
	4	10.75	10.85
		Average 10.8 at. % Li ± .1	
3	1	6.77	6.83
	2	6.89	6.93
	3	6.69	6.79
	4	6.87	6.88
		Average 6.8 at. % Li ± .1	

8.32×10^{-6} per sec. Stresses were determined to within $\pm 2 \times 10^{6}$ dynes/cm^2 and tensile strains were measured to within $\pm$ 0.0001.

III. EXPERIMENTAL RESULTS

The experimental results of the three compositions will be given in the order of 12.5, 10.8 and 6.8 at.% Li, respectively.

12.5 at.% Li

The values of resolved shear stress vs resolved shear strain for different temperatures are plotted in Fig. 2. Whereas pure Mg oriented for prismatic slip exhibited brittle behavior below 450°K, the 12.5 at.% Li-Mg undertook more than 30% resolved shear strain at 4°K and fractured before the initiation of duplex slip. All crystals except the ones tested at 4°K fractured on the prismatic planes upon initiation of duplex slip and showed about 70% resolved shear strain. They clearly show a yield phenomenon at lower temperatures and a rather modest rate of strain hardening which increases somewhat with a decrease in the test temperature. The temperature dependence of the critical resolved shear stress, as shown in Fig. 3, established the fact that the critical resolved shear stress was nearly temperature independent in the region of 300 to about 400°K for shear strain rate $\dot{\gamma} = 1.66 \times 10^{-4}$/sec, and varied only modestly and parallel to the change in shear modulus G with temperature as given by Roberts.[8] The thermally activated component of the stress, τ^*, was deduced from the relationship; $\tau^* = \tau_T - \tau_r \frac{GT}{Gr}$ in order to obtain a reproducible data from each crystal. G_T and G_r are the shear moduli at temperature T and the temperature of reference respectively. τ_T is the total stress required to cause plastic flow at temperature T and can generally be shown as the sum of two factors:

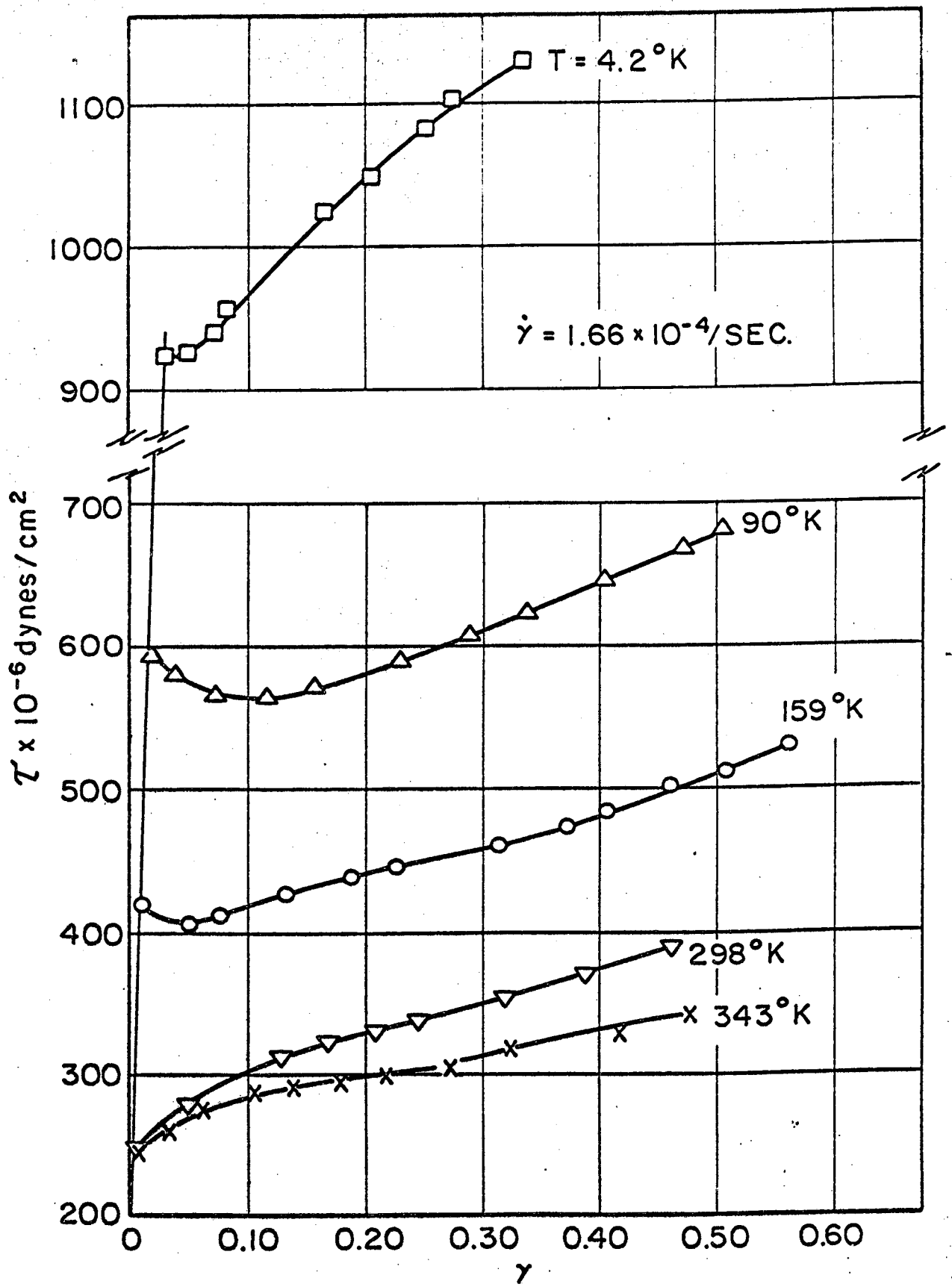

FIG. 2 RESOLVED SHEAR STRESS vs. RESOLVED SHEAR STRAIN FOR PRISMATIC SLIP IN 12.5 AT.% Li-Mg.

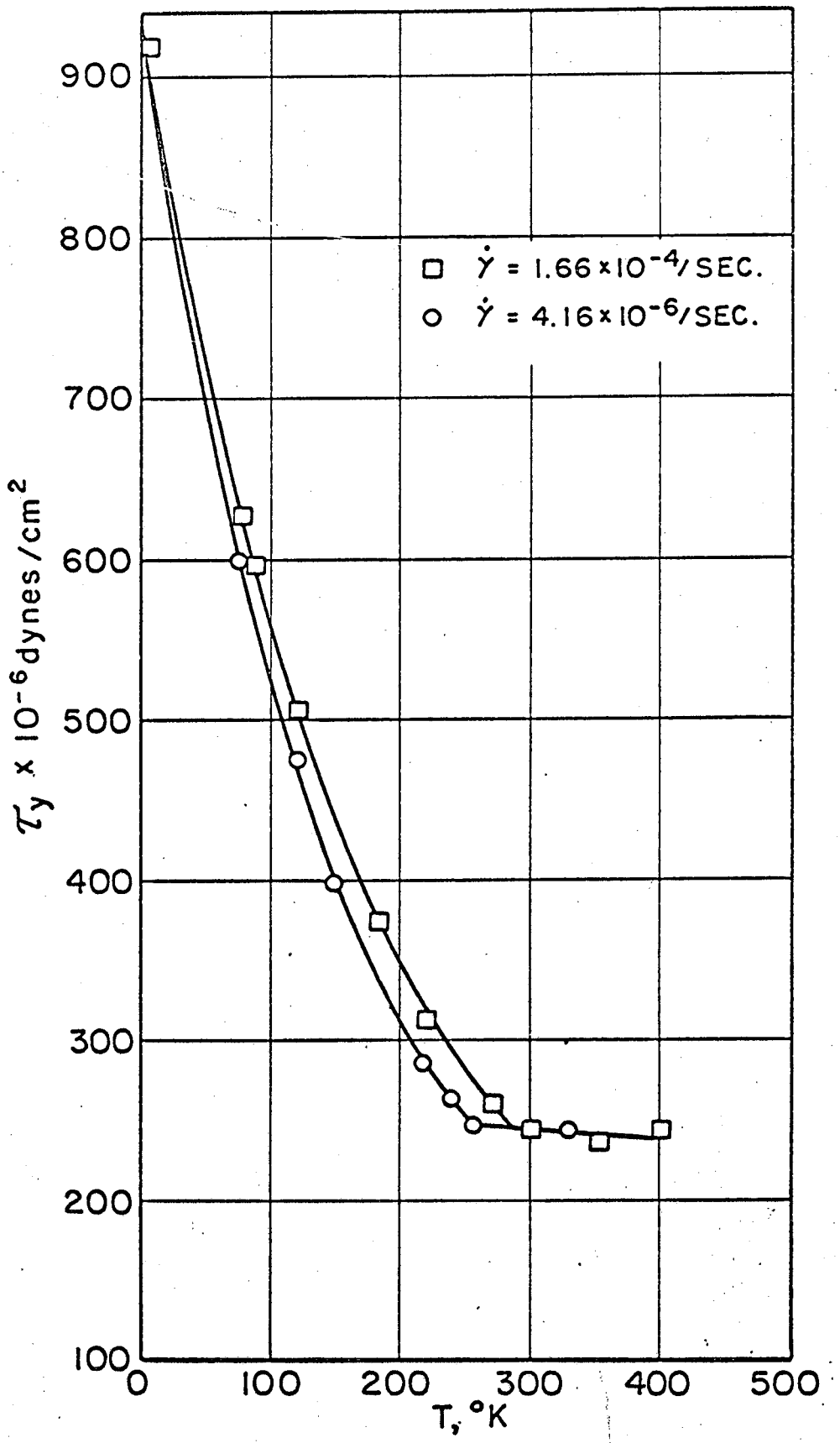

FIG.3 CRITICAL RESOLVED SHEAR STRESS vs. TEMPERATURE FOR PRISMATIC SLIP IN 12.5AT.% Li-Mg.

$$\tau = \tau^* + \tau_A$$

where τ^* is the component of the stress that is needed to help dislocations to surmount barriers over which they move with the aid of thermal fluctuations, and τ_A is the component of the stress that must be supplied to push the dislocations over such barriers as cannot be surmounted by thermal fluctuations. Here τ^* decreases rather rapidly with an increase in temperature whereas τ_A decreases in a manner that parallels the decrease in the shear modulus of elasticity, G, with temperature. For the convenience of the experimental procedures, the temperature of reference r was taken 300°K for $\dot{\gamma} = 1.66 \times 10^{-4}$/sec and 273°K for $\dot{\gamma} = 4.16 \times 10^{-6}$/sec.

The effect of strain rate on stress at a given temperature is shown by the parameter "β" in Fig. 4, where β is defined as:

$$\beta = \left(\frac{\partial \ln \dot{\gamma}}{\partial \tau}\right)_T \simeq \left(\frac{\ln \dot{\gamma}_2 - \ln \dot{\gamma}_1}{\tau_2 - \tau_1}\right)_T$$

where

$\dot{\gamma}$ = the shear strain rate

τ = the shear stress and

T = the absolute temperature

These data were obtained by measuring the change in resolved shear stress, $\tau_2 - \tau_1$, upon changing the shear strain rate from $\dot{\gamma}_1$ to $\dot{\gamma}_2$ by a factor of 10 times. β decreased to a minimum at about 140°K and then increased to a very large value at the neighborhood of room temperature.

The apparent activation volume, which will be used subsequently, defined as the parameter $\beta kT = \frac{\ln \dot{\gamma}_2 - \ln \dot{\gamma}_1}{\tau_2 - \tau_1} kT$ was a function of

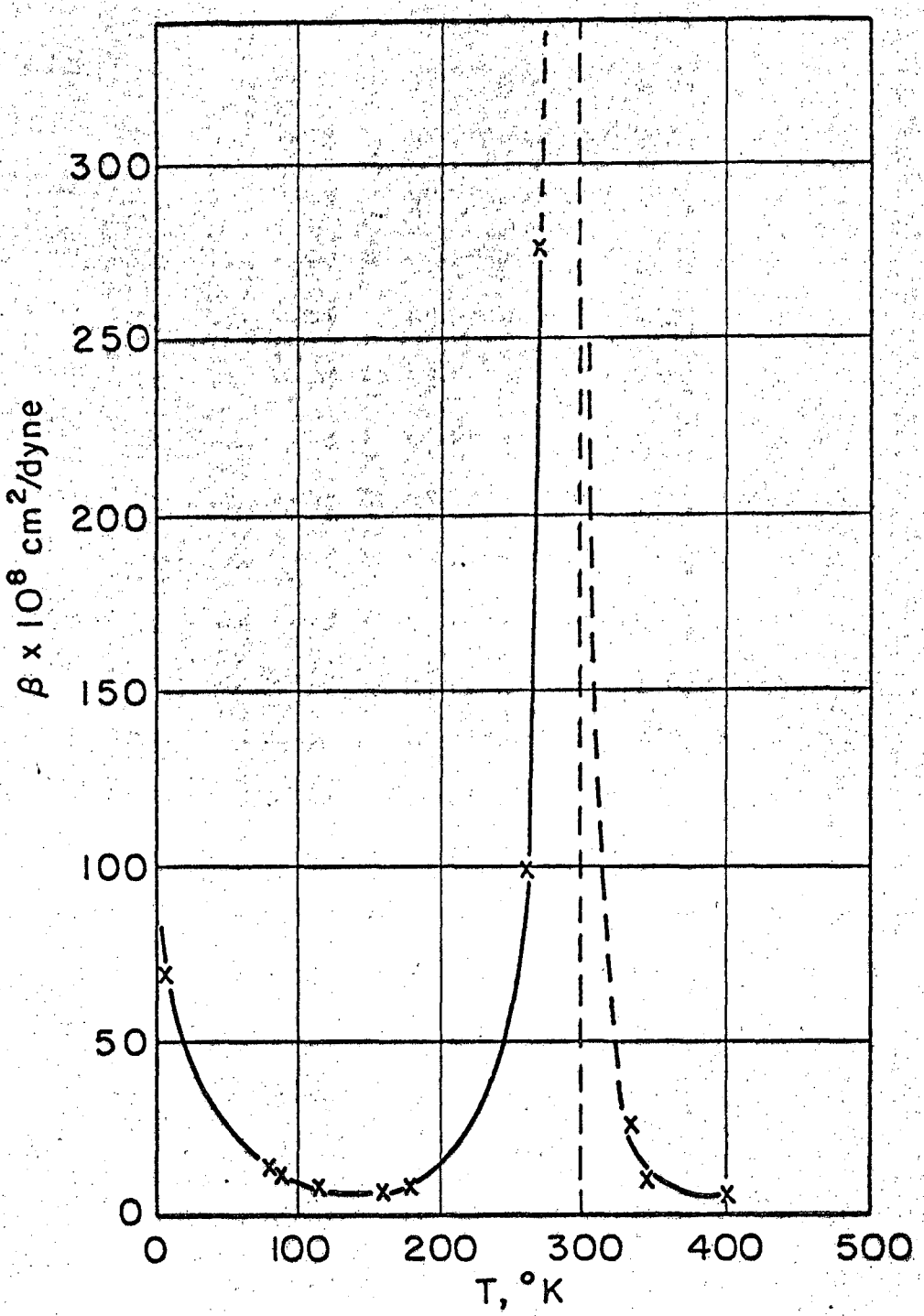

β vs. TEMPERATURE FOR 12.5 AT.% Li-Mg.

FIG. 4

temperature and increased linearly at lower temperatures then increased precipitously with temperature reaching a very large value at the neighborhood of room temperature where flow stress becomes strain rate independent. This effect is shown in Fig. 5 in order to reveal the stress sensitivity of the strain rate. The activation volume appears to increase with temperature but remains relatively insensitive to the strain as shown in Fig. 6.

10.8 at.% Li

A somewhat similar set of data were obtained from the 10.8 at.% Li alloy of Mg and Figs. 7 through 11 show the various effects discussed in the previous section. The crystals undergo plastic deformation at temperatures as low as 4.2°K and fracture on the prismatic planes upon initiation of duplex slip. They introduced a less pronounced yield phenomenon at low temperatures and probably a lower rate of hardening. The temperature independent region of the critical resolved shear stress was found to be from 325 to about 380°K for the shear strain rate $\dot{\gamma} = 1.66 \times 10^{-4}$/sec and the same technique as used in the 12.5 at.% alloy was also used to adjust for the specimen variation. The reference temperatures used for this purpose were 300 and 325°K for the shear strain rates of 4.16×10^{-6} and 1.66×10^{-4}/sec, respectively.

The effect of strain rate for a constant 10 to 1 change on the stress with the variation of temperature is shown on Fig. 9 and it has in general a similar shape as Fig. 4. The apparent activation volume is a function of temperature increasing linearly at low temperatures and then precipitously at higher temperatures reaching a very large value around 320°K as shown in Fig. 10. The variation of the apparent activation volume with shear strain is represented in Fig. 11 as a function of the temperature.

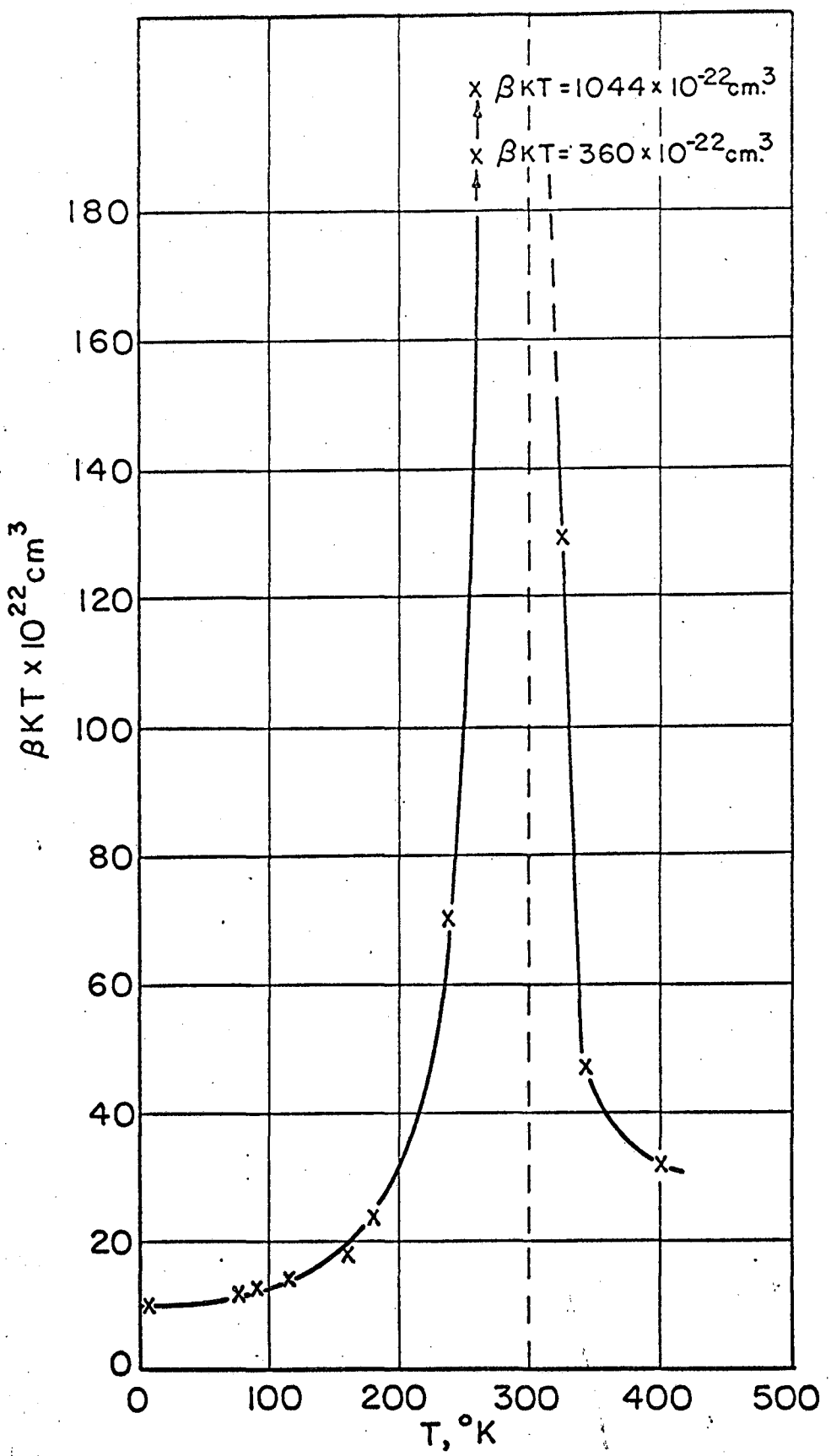

FIG. 5 APPARENT ACTIVATION VOLUME "βKT" vs. T°K FOR 12.5AT.% Li-Mg.

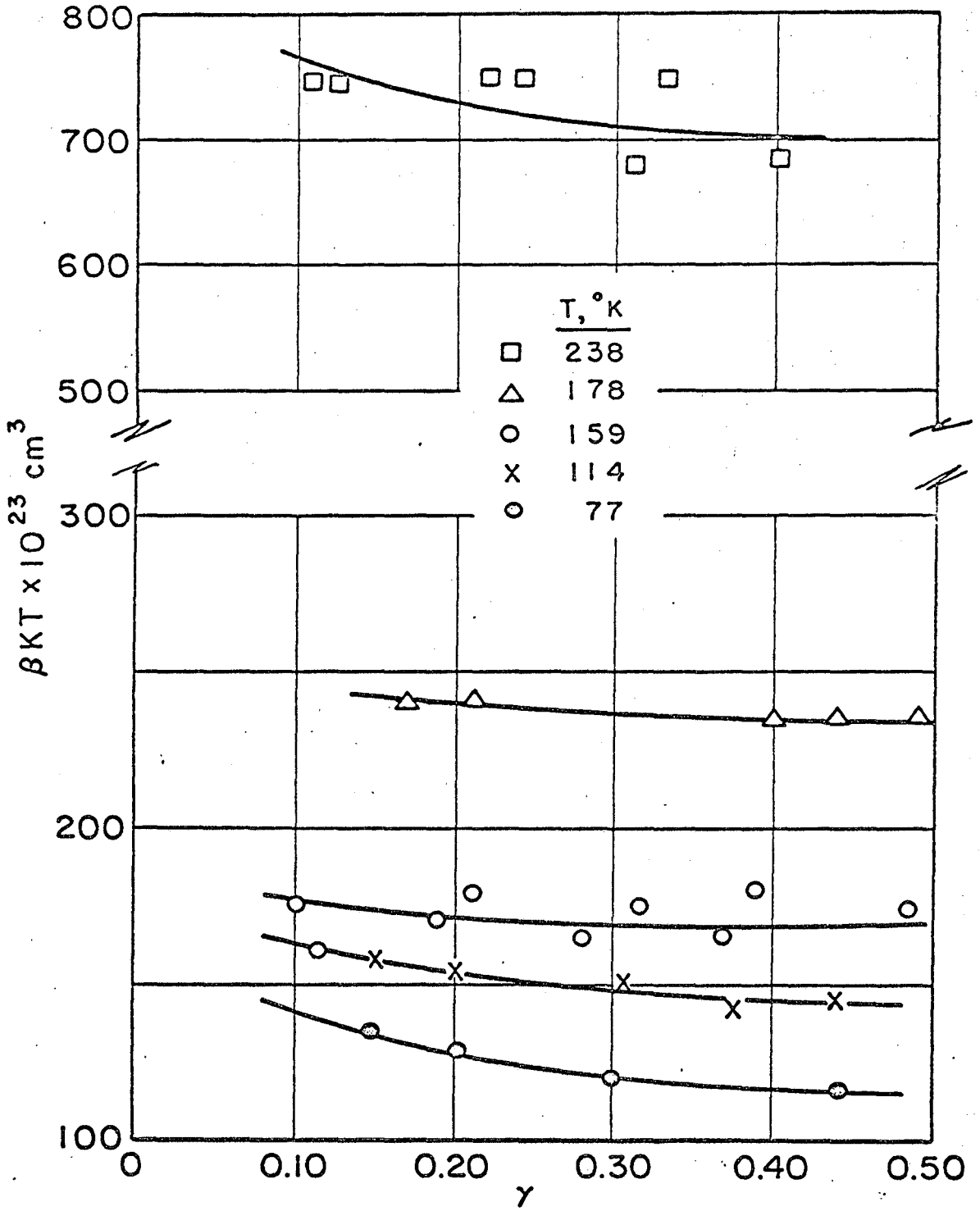

FIG.6 APPARENT ACTIVATION VOLUME, βKT vs. RESOLVED SHEAR STRAIN FOR 12.5AT.% Li-Mg.

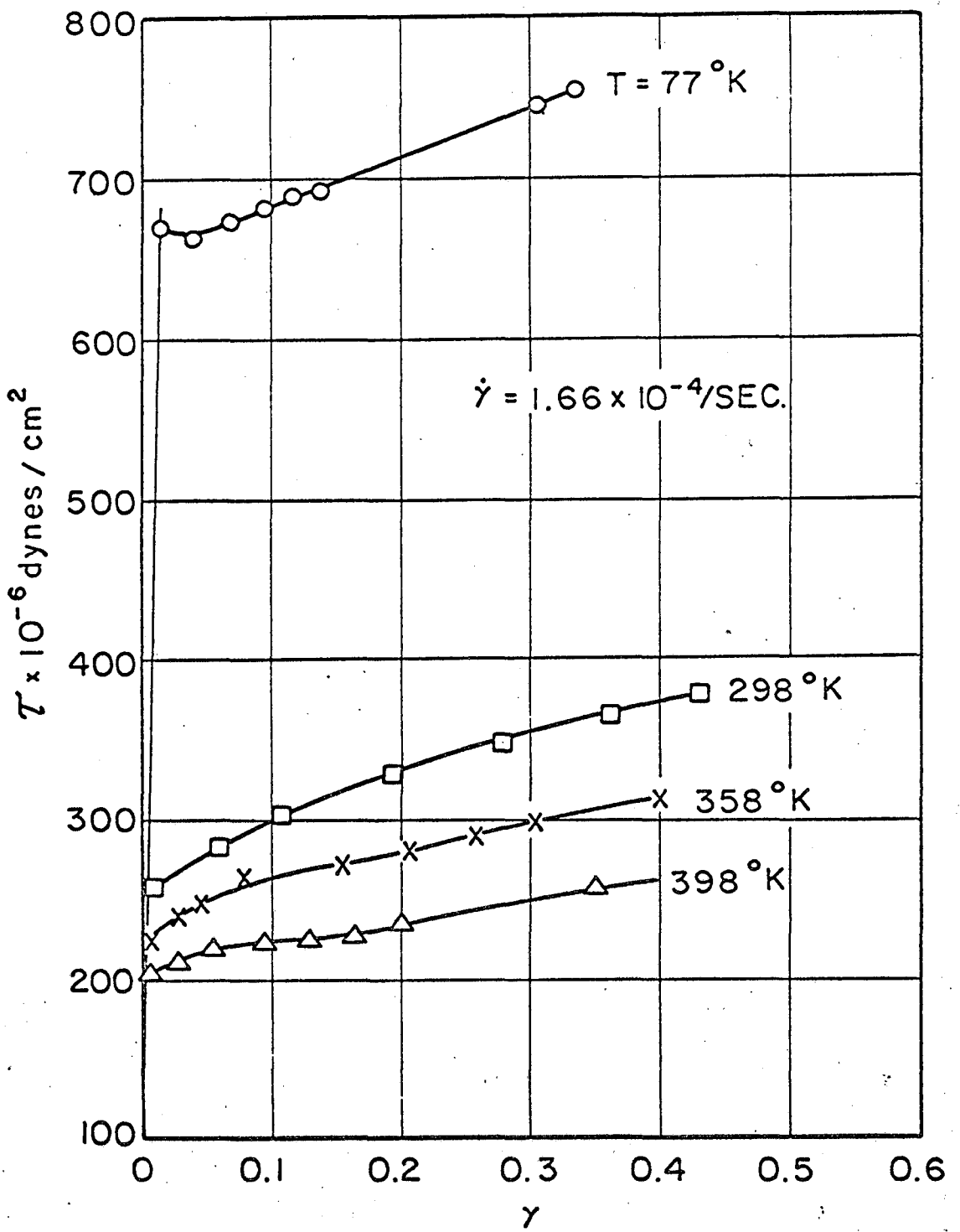

FIG.7 RESOLVED SHEAR STRESS vs. RESOLVED SHEAR STRAIN FOR PRISMATIC SLIP IN 10.8 AT.% Li-Mg.

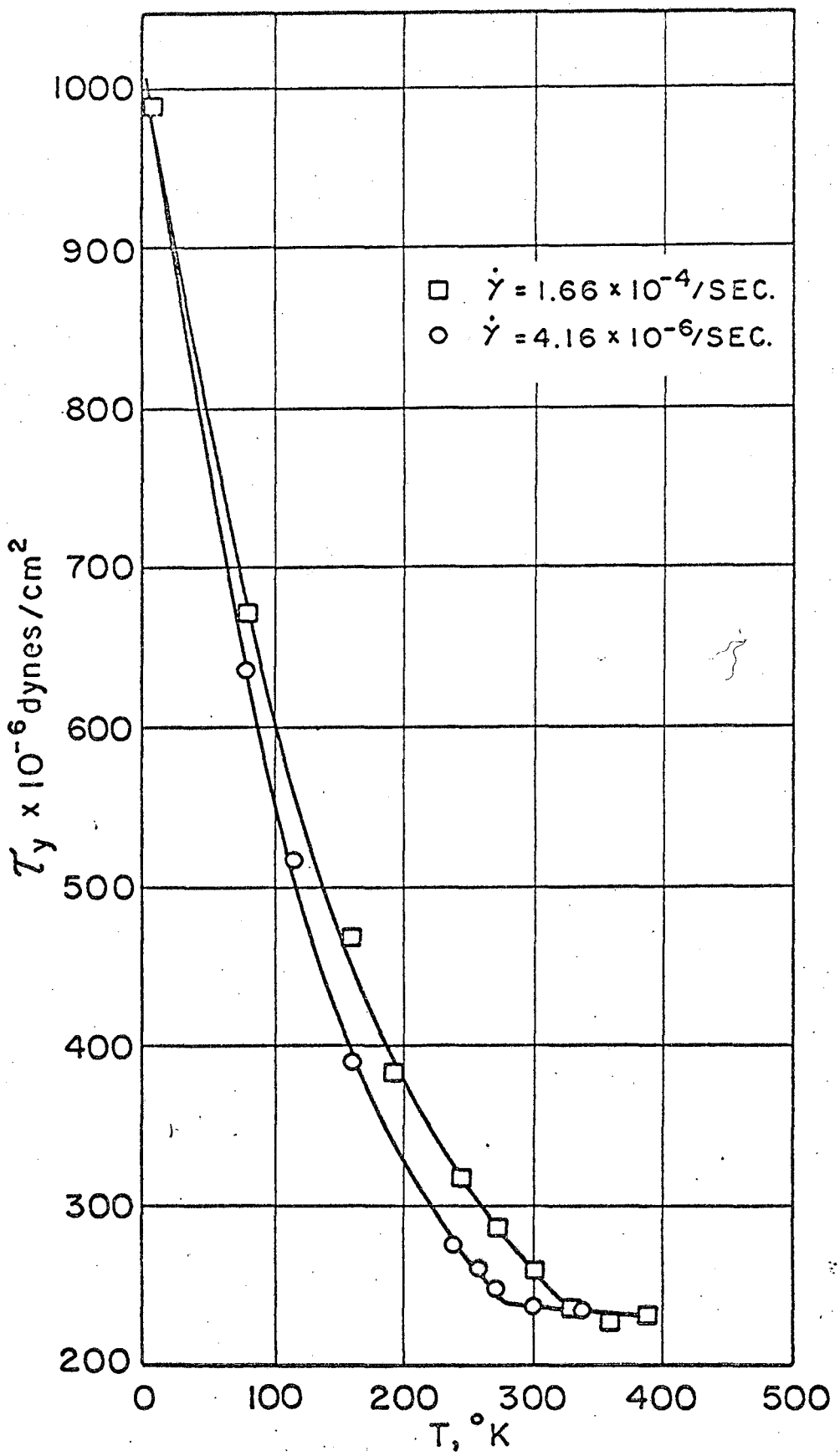

FIG. 8 CRITICAL RESOLVED SHEAR STRESS vs. TEMPERATURE FOR PRISMATIC SLIP IN 10.8 AT.% Li-Mg

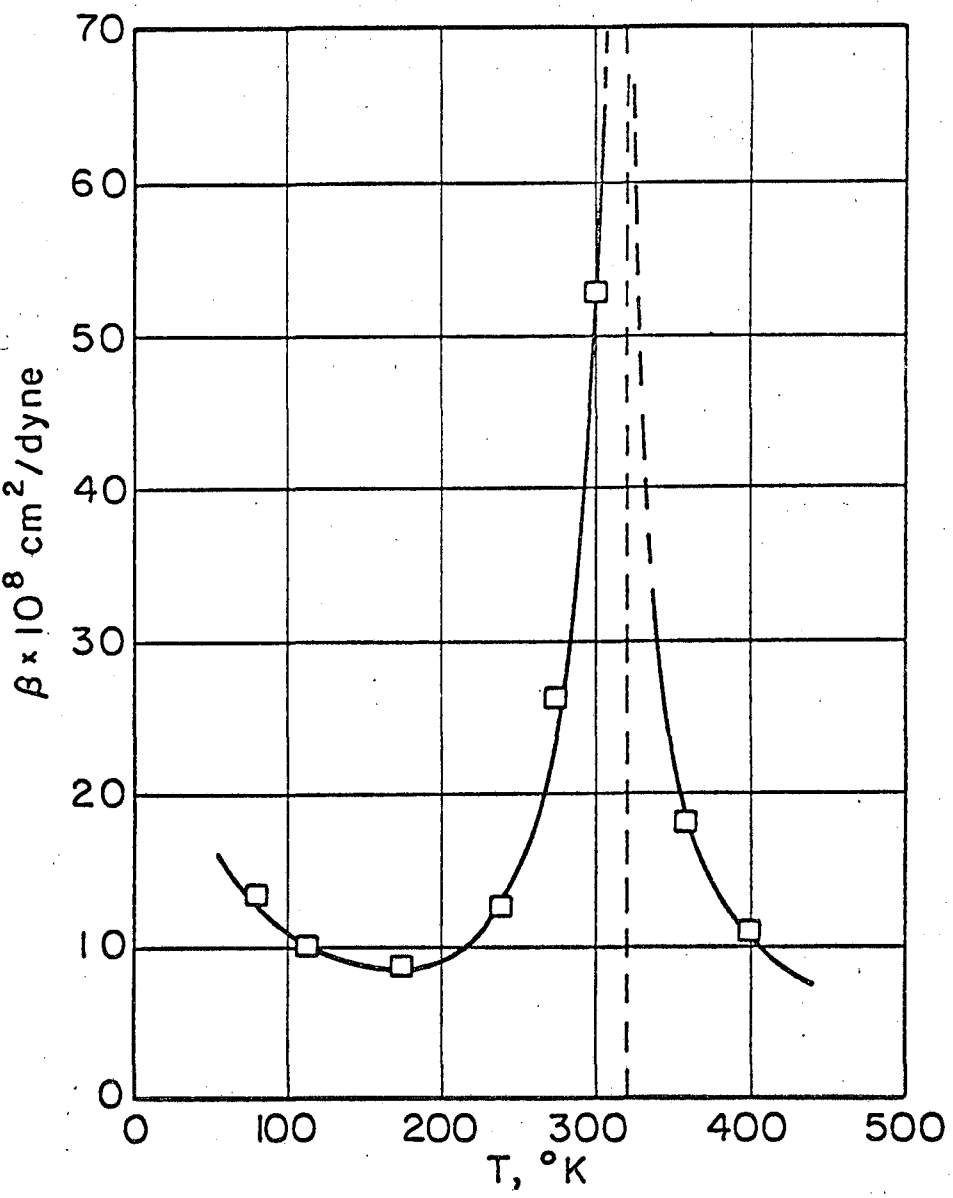

β vs. TEMPERATURE
FOR 10.8 AT.% Li-Mg.

FIG. 9

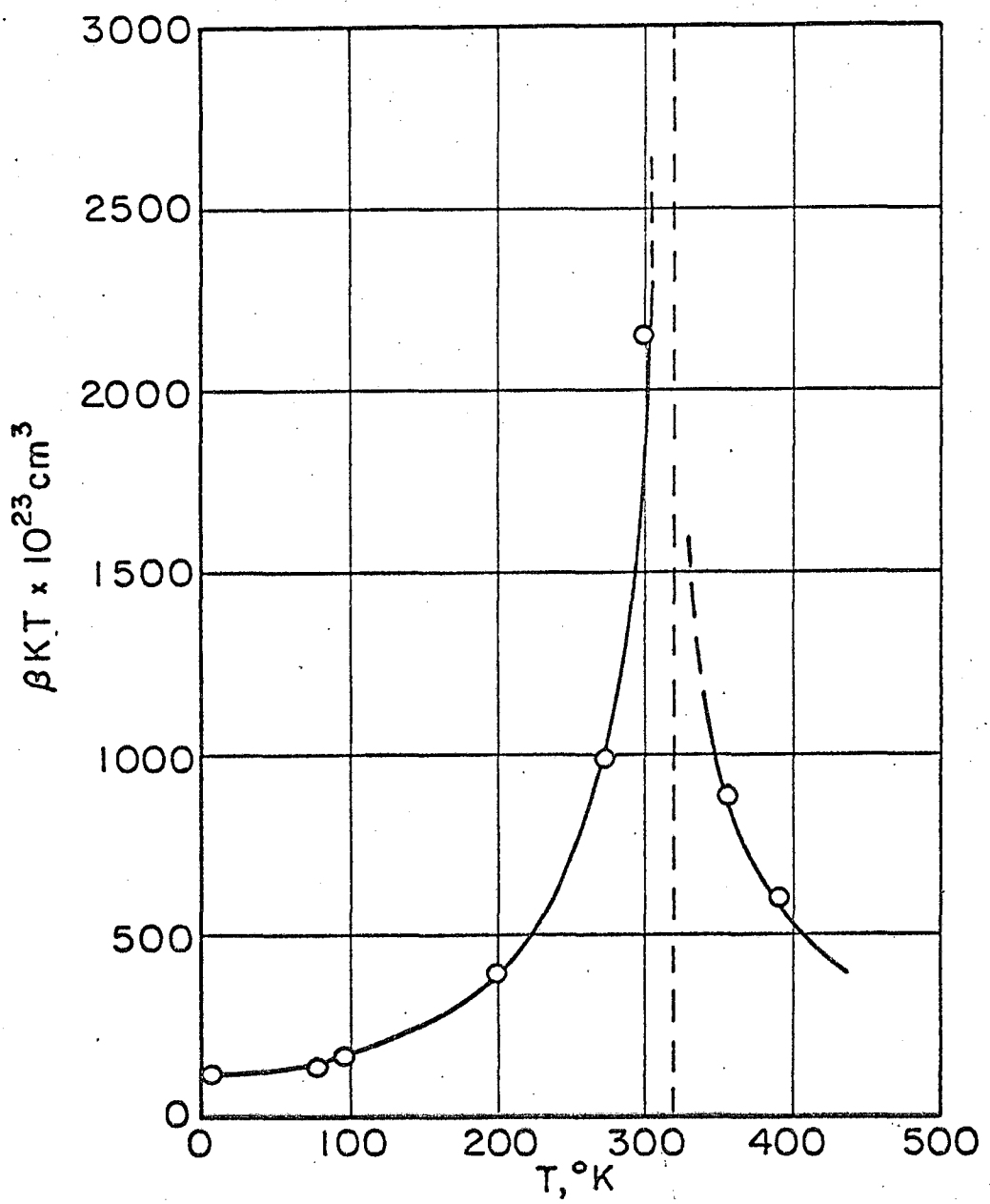

FIG. 10 APPARENT ACTIVATION VOLUME, "βKT," vs. TEMPERATURE FOR 10.8 AT.% Li-Mg.

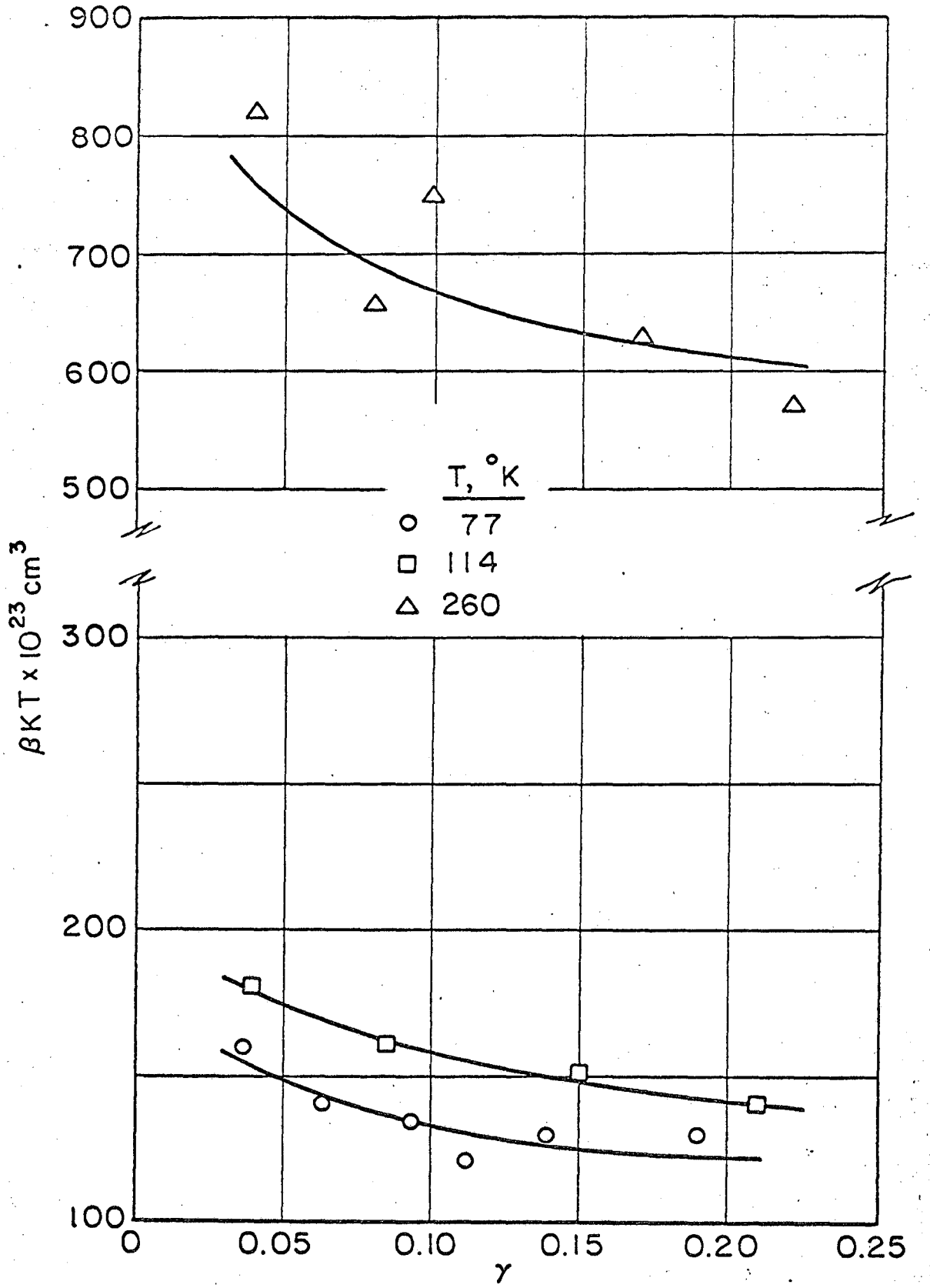

FIG. 11 APPARENT ACTIVATION VOLUME, "βKT," vs. RESOLVED SHEAR STRAIN FOR 10.8 AT.% Li-Mg.

6.8 at.% Li

Figure 12 shows the temperature dependence of the strain hardening for this composition. Although the rate of hardening is similar to those shown by the other two alloys at low temperatures, there is almost no strain hardening at high temperatures. The pronounced yield phenomenon shown by the 12.5 at.% alloy which was smaller in the 10.8 at.% alloy is not present in this alloy.

The plot of critical resolved shear stress vs temperature given in Fig. 13 shows a different phenomenon from the ones obtained for the higher Li content alloys. No plastic deformation took place below 200°K and prismatic slip was preceeded by twinning and fracturing. The critical resolved shear stress was strongly temperature dependent in the region between about 210 and 350°K, less temperature dependent in the vicinity of 350-500°K, and again temperature dependent above 500°K.

The variation of "β" and apparent activation volume "βkT" with temperature are shown in Figs. 14 and 15, respectively. The dependence of the activation volume on temperature undergoes similar changes to those discussed for the critical shear stress; it is very small and almost temperature independent at low temperatures and it increases markedly at temperatures higher than 550°K.

IV. DISCUSSION

This discussion will be divided into three sections; 12.5 at.%, 10.8 at.% and 6.8 at.% Li and discussed separately. Later a discussion will be given of the combined results and conclusions will be drawn.

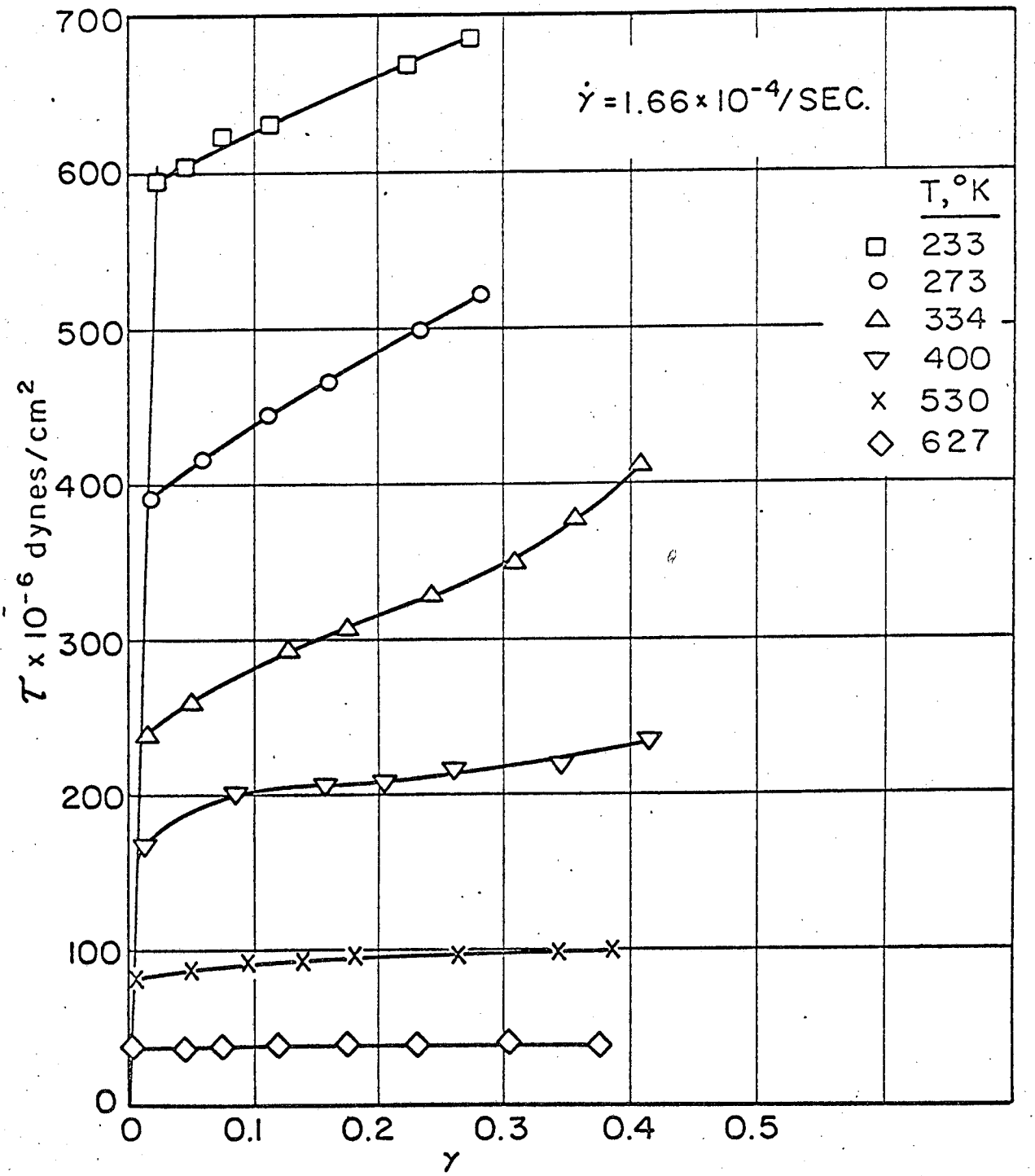

FIG. 12 RESOLVED SHEAR STRESS vs. RESOLVED SHEAR STRAIN FOR PRISMATIC SLIP IN 6.8 AT.% Li-Mg.

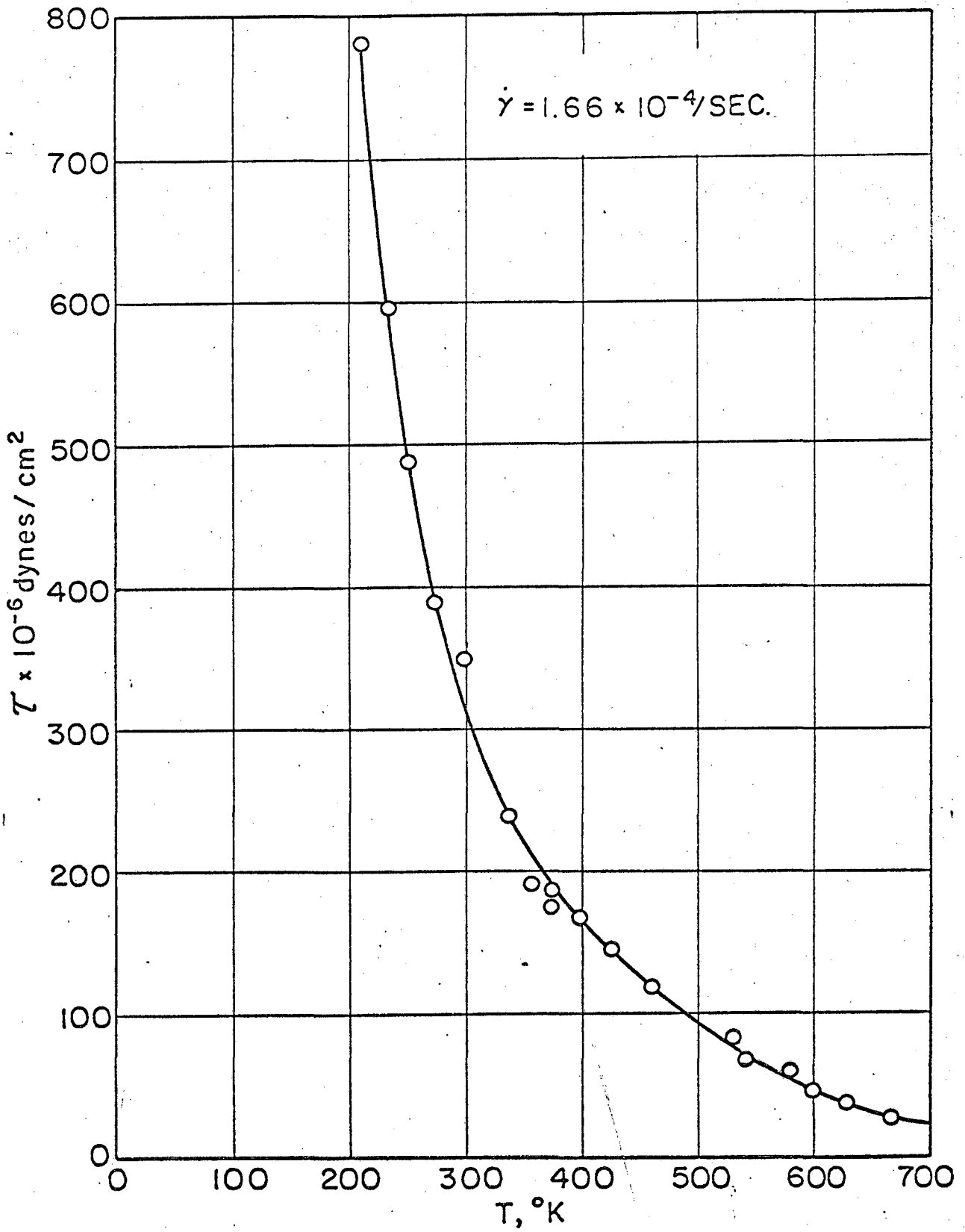

FIG. 13 CRITICAL RESOLVED SHEAR STRESS vs. TEMPERATURE FOR PRISMATIC SLIP IN 6.8 AT. % Li-Mg.

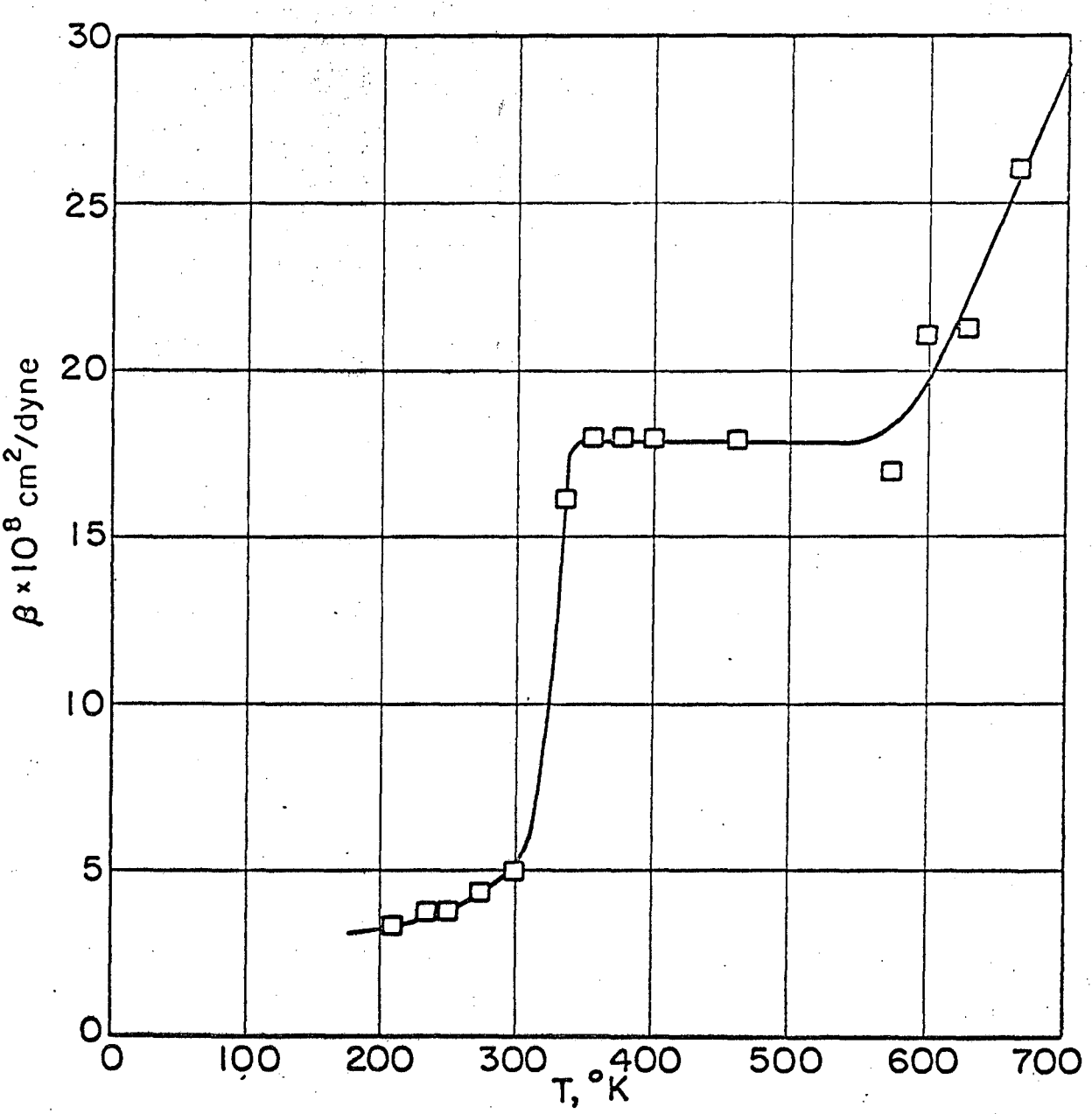

FIG. 14 β vs. TEMPERATURE FOR 6.8 AT.% Li-Mg.

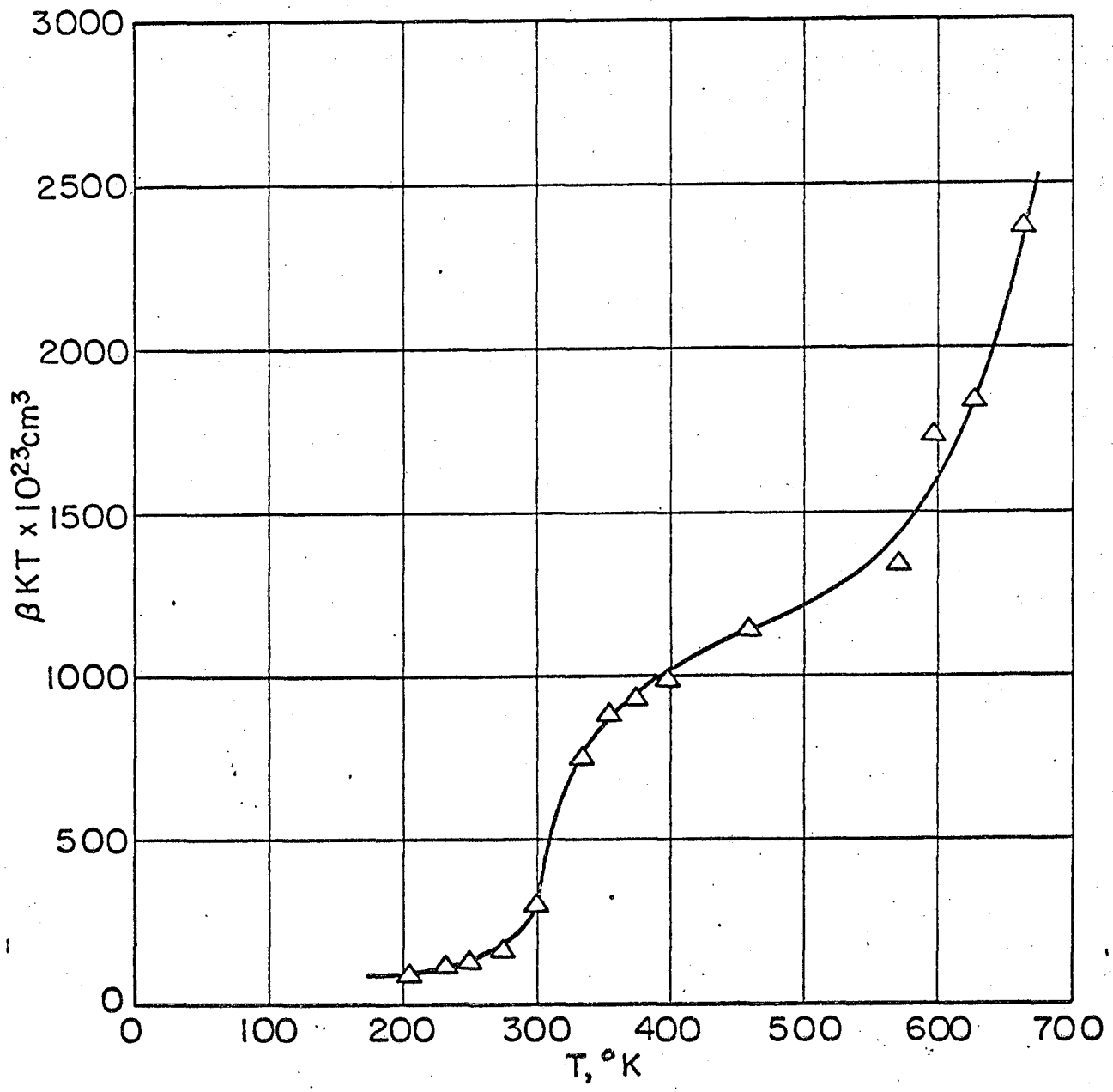

FIG. 15 APPARENT ACTIVATION VOLUME, "βKT," vs. TEMPERATURE FOR 6.8AT.% Li-Mg.

12.5 at.% Li

It will be shown that among the various processes that might be responsible for the rate of prismatic slip in Mg-Li alloy of 12.5 at.% Li, Peierls' process is obviously the one which is more likely to be the rate controlling mechanism at low temperatures.

At first the other two possible processes, namely, intersection and cross-slip will be ruled out and then we will show that Peierls' mechanism agree well with the data.

According to Basinski's[14] modification of the Seeger[15] theory for intersection of dislocations,

$$\dot{\gamma} = n \ell^2 b \nu_o e^{-U_i/kT} \tag{1}$$

where

n = the number of points per unit volume where intersection can occur

ℓ = the mean spacing of the forest dislocations

U_i = the activation energy for intersection

$$= \int_F^{F_{max}} x dF$$

F_{max} = the maximum force necessary to affect intersection

x = the distance through which a dislocation must move to complete intersection

$F = \tau \ell b$ = the force assisting thermal activation.

For intersection:

$$\beta = -\frac{1}{kT}\left(\frac{\partial U_i}{\partial \tau}\right) = \frac{\ell b x}{kT} \tag{2}$$

where ℓbx is a function of the applied stress τ. Once constriction of the forest dislocation is complete τ should increase rapidly with decreasing $x\ell b$ at a value of $x \simeq b$. When this is applied to the experimental data given in Fig. 16, it suggests that $\ell b^2 < 1.5 \times 10^{-21} cm^3$. Consequently, the density of forest dislocations estimated in this way has the value of,

$$\rho = \frac{1}{\ell^2} > 4.5 \times 10^{11}.$$

For an unworked crystal this is several order of magnitude higher than that determined by other methods or that usually observed in the electron microscope.

The observed results also disagree with Friedel's concept that prismatic slip rate is determined by the rate of nucleation of cross-slip.[16] Friedel's theory assumes that dislocations containing edge components slip with ease on the prismatic plane until they traverse the entire plane, combine with dislocations of opposite sign or become blocked. Such blocking can occur in the vicinity of screw dislocations which automatically dissociate with a decrease in energy into their partials on the basal plane. Continued slip, therefore, requires continued recombination of the partials on the basal plane to form screw dislocations on the prismatic plane. Friedel has shown that the activation energy for nucleation of cross-slip is given by

$$U = U_c + \frac{2^{5/2} R^{3/2} \Gamma^{1/2}}{3\tau b} \qquad (3)$$

where

U_c = the energy to form a constriction in the partials on the basal plane

R = the energy to recombine a unit length of the two partials.

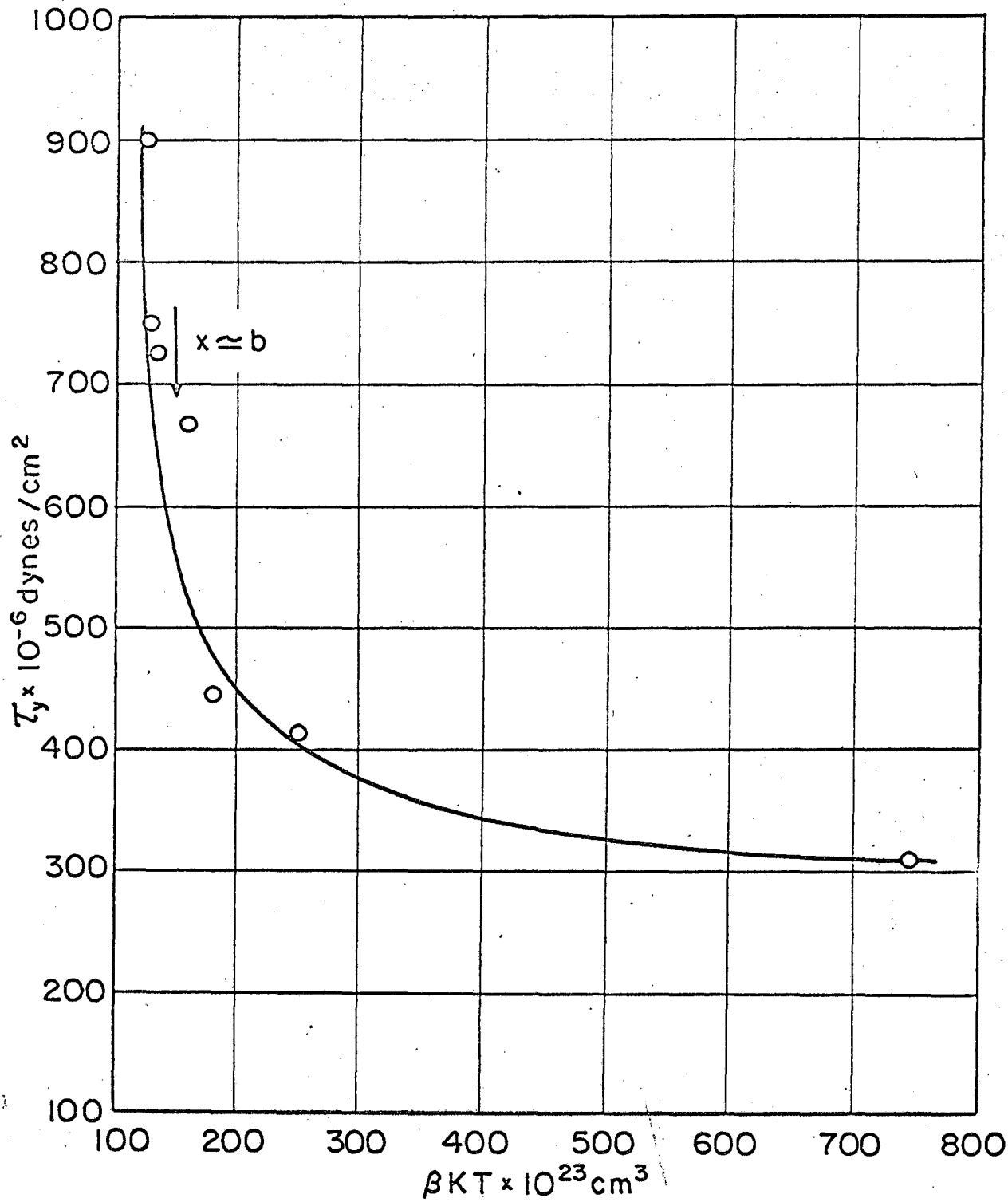

FIG. 16 CRITICAL RESOLVED SHEAR STRESS vs. APPARENT ACTIVATION VOLUME FOR 12.5 AT.% Li-Mg.

Both U_c and R are constants in the present case since the resolved shear stress on the basal plane was always zero, and therfore, the partials were separated by the equilibrium spacing under zero stress.

The shear strain rate for prismatic slip is given by the usual expression:

$$\dot{\gamma} = nAb\nu \exp - \frac{U}{kT}$$

where

n = the number of points per unit volume at which cross-slip can occur,

A = the average area swept out per process

$\nu = \nu_o b/y$ = the frequency of cross slip, where

$y = \frac{2^{3/2}(R\Gamma)^{1/2}}{\tau b}$ and

$n = \lambda/y$, where

λ = the total length per unit volume of screw dislocations on the operative prismatic plane.

Then for Friedel's mechanism the shear strain rate is given by

$$\dot{\gamma} = \frac{\lambda Ab^4 \nu_o \tau^2}{8k\Gamma} \exp - \frac{U_c}{kT} \exp - \frac{2^{5/2} R^{3/2} \Gamma^{1/2}}{3kT\tau b} \tag{4}$$

which upon rearrangement gives

$$\frac{1}{\tau T} = \frac{3bK}{2^{5/2} R^{3/2} \Gamma^{1/2}} \ln \frac{\lambda Ab^4 \nu_o}{8R\Gamma\dot{\gamma}} + \frac{3bK\tau}{2^{3/2} R^{3/2} \Gamma^{1/2}} - \frac{3bU_c}{2^{5/2} R^{3/2} \Gamma^{1/2}} \tag{5}$$

Since the first terms to the right of the equality is a constant and the second term varies only modestly with the applied shear stress, $\frac{1}{\tau T}$ should decrease almost linerally with $\frac{1}{T}$. The experimental

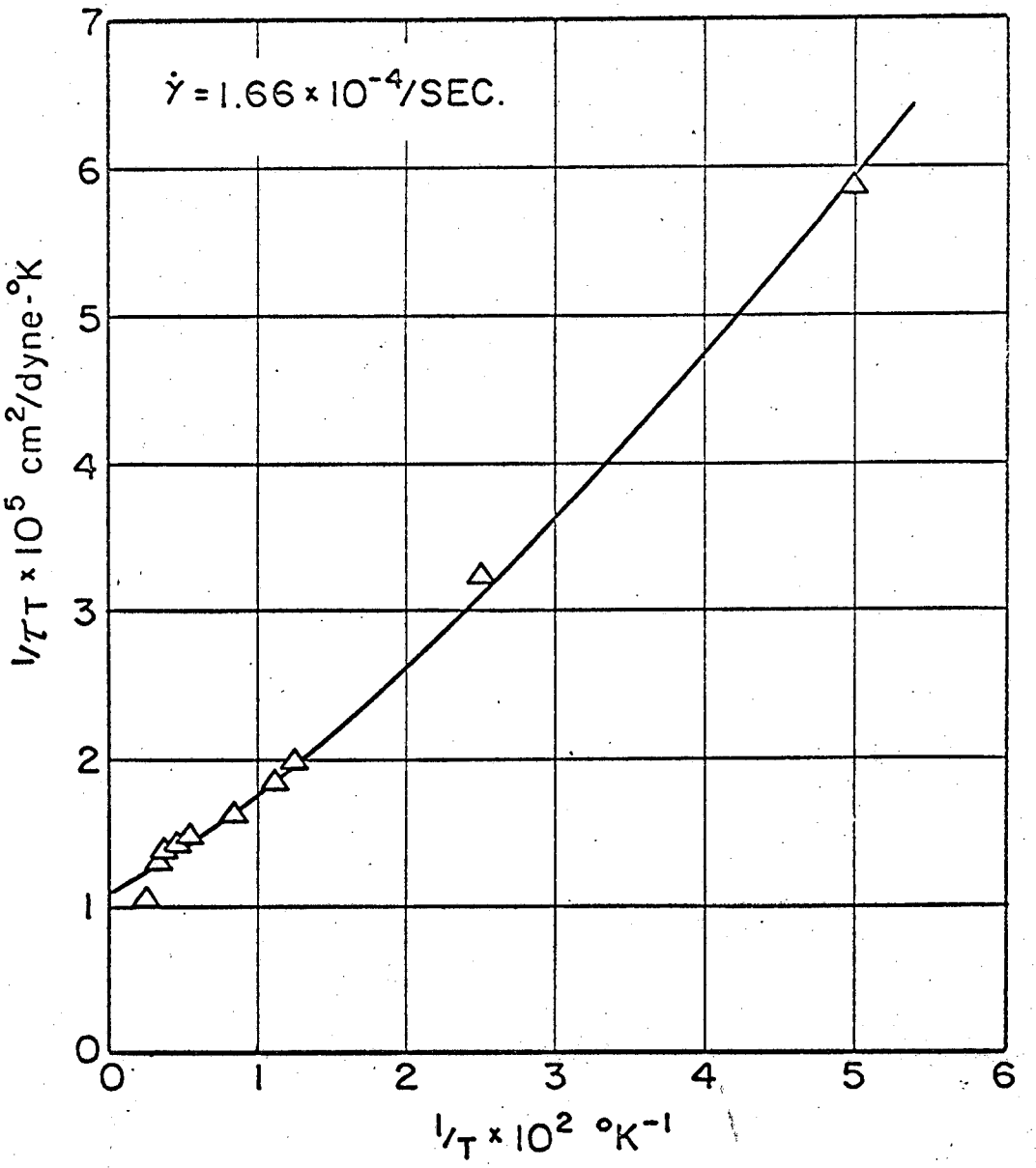

FIG. 17 THE PLOT OF $1/\tau T$ vs. $1/T$ FOR PRISMATIC SLIP IN 12.5 AT. % Li-Mg.

results represented in Fig. 17 show that $\frac{1}{\tau T}$ increases with $\frac{1}{T}$. Consequently, cross-slip is also ruled out as the rate controlling mechanism.

Having concluded that neither the cross-slip nor the intersection mechanism can be the rate controlling mechanism, we shall now show that the experimental observations are in excellent agreement with Peierls' process which postulates that the thermal activation of a dislocation from one potential well to the adjacent potential well in the slip plane is rate controlling.

A. Effect of Temperature and Strain-Rate on Flow Stress

The values of τ^* for two strain rates taken from Fig. 3 corrected for change in shear modulus with temperature $\frac{G_o}{G_T}$,[8] are shown in Fig. 18. It is apparent from Fig. 18 that there is a critical temperature, depending on the strain rate, where the thermally activated process changes to an athermal process. Calling these temperatures T_{c_1}, and T_{c_2} for the slower and faster strain rates, respectively. The shape of the τ^* vs T curves agree well with those that Dorn and Rajnak[17] have predicted when plastic flow arises from the nucleation of pairs of kinks by the Peierls' mechanism.

We will now compare quantitatively the experimental results with the theory for deformation controlled by the nucleation of pairs of kinks. For the simplest case where the deformation rate is controlled by the nucleation of pairs of kinks in a geometrically determined length L of dislocations,[17]

$$\dot{\gamma} = \rho ab\nu \frac{L}{w} e^{-\frac{U_n}{kT}} \tag{6}$$

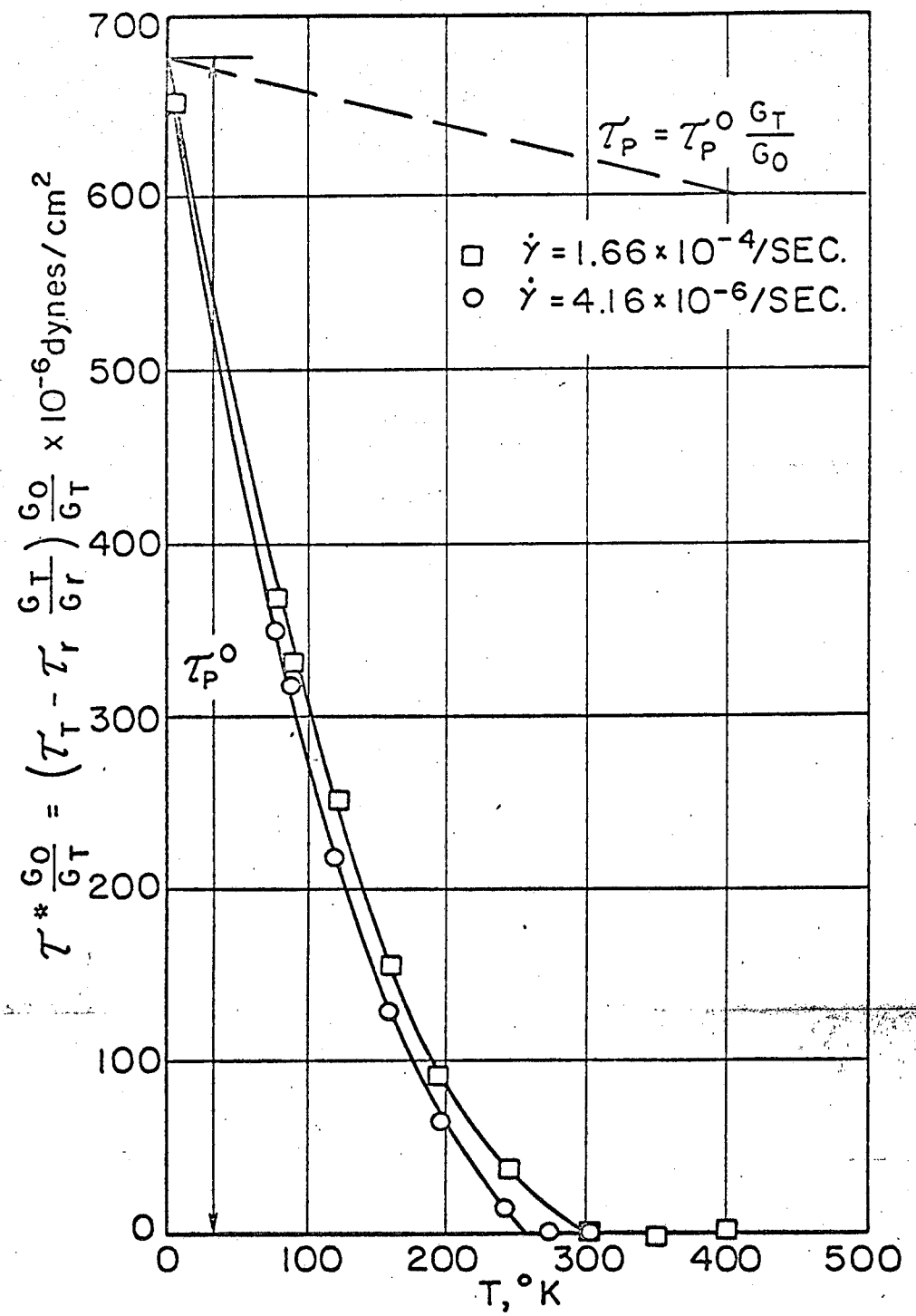

FIG. 18 THERMALLY ACTIVATED COMPONENT OF FLOW STRESS τ^* vs. TEMPERATURE IN 12.5 AT.% Li-Mg.

where

ρ = the density of freely mobile dislocations,

a = the distance between the Peierls valleys

b = the Burgers vector

ν = the Debye frequency

w = the width of a pair of kinks at the saddle point free energy configuration

U_n = the saddle-point free energy for the nucleation of a pair of kinks

k = the Boltzmann constant and

T = the absolute test temperature

The theory gives $U_n/2U_k$ as a function of τ^*/τ_p, as shown by the curves of Fig. 19, where

U_k = the kink energy and

τ_p = the Peierls

for each of a series of values of α where α expresses the deviation of the shape of the Peierls hills from a sinusoidal periodic variation. The shape of the Peierls Hill was defined in terms of α by

$$\Gamma(y) = \left(\frac{\Gamma_c + \Gamma_o}{2}\right) + \left(\frac{\Gamma_c + \Gamma_o}{2}\right) \cos \pi \frac{1}{a} + \frac{\alpha\left(\Gamma_c + \Gamma_o\right)}{4}\left(1 - \cos \frac{4\pi y}{a}\right)$$

where Γ_c is the line energy of a dislocation at the top of the Peierls hill where y = 0, Γ_o is the energy in the valley where y = ± a/2 and Γ (y) is the energy when the dislocation is displaced a distance y from the top of the hill. At $T = T_c$ where τ^* first becomes zero, the thermal energy that need be supplied is just $U_n = 2U_k$, and therefore, for this condition,

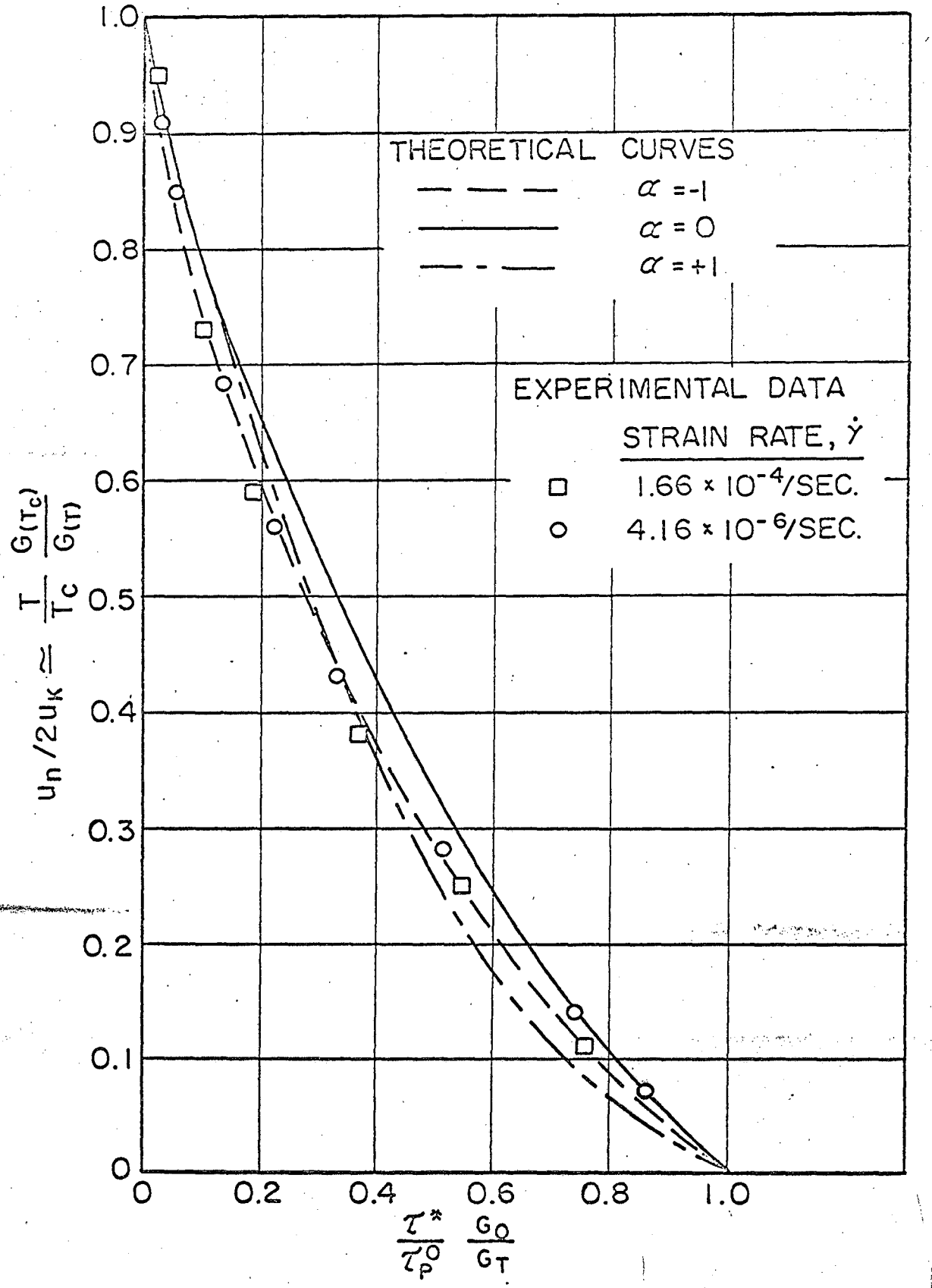

FIG. 19 THERMALLY ACTIVATED FLOW STRESS vs. TEMPERATURE IN DIMENSIONLESS UNITS FOR 12.5AT.% Li-Mg.

$$\dot{\gamma} = \rho ab\nu \frac{L}{w_c} e^{-\frac{2U_k}{kT_c}} \tag{7}$$

But, as shown by Dorn and Rajnak, to a very good approximation $w \simeq w_c$ and therefore, as shown by Eqs. 6 and 7

$$\frac{U_n}{2U_k} = \frac{U_n}{2U_k \frac{G(T)}{G(T_c)}} \simeq \frac{T}{T_c} \frac{G(T_c)}{G(T)} \tag{8}$$

Furthermore, taking as required by theory that the Peierls stress at the absolute zero τ_p° is τ^* at the absolute zero, we obtain $\tau_p^\circ = 6.80 \times 10^8$ dynes/cm^2. Assuming that the Peierls stress decreases with increasing temperature in the same manner as the shear modulus decreases we can write

$$\tau_p = \tau_p^\circ \frac{G(T)}{G(O)} \tag{9}$$

which is shown by the broken line at the top of Fig. 18. The experimental data $U_n/2U_k$ as a function of $\frac{\tau^*}{\tau_p}$ as deduced with the aid of Eqs. 8 and 9 are shown by the points given in Fig. 19. The theoretical trends as shown by the solid curves in Fig. 19 are in good agreement with the experimental data and it appears to agree best with the curve representing $\alpha = -1$.

B. Activation Energy for Nucleation of Pairs of Kinks

The activation energy can be determined if the change in strain rate due to change in temperature of constant stress is known. From Eq. 7

$$\frac{\dot{\gamma}_2}{\dot{\gamma}_1} = \frac{e^{\frac{-2U_k}{kT_{c_2}} \frac{G(T_{c_2})}{G(O)}}}{e^{\frac{-2U_k}{kT_{c_1}} \frac{G(T_{c_1})}{G(O)}}} . \tag{10}$$

or

$$2U_k = \frac{KG(O)}{\frac{G(T_{c_1})}{T_{c_1}} - \frac{G(T_{c_2})}{T_{c_2}}} \times \frac{\dot{\gamma}_2}{\dot{\gamma}_1}$$

using

$$K = 1.38 \times 10^{-16} \text{erg/degree}$$

$$G(O) = 1.855 \times 10^{11} \text{dynes/cm}^2$$

$$G(T_{c_1}) = 1.720 \times 10^{11} \text{dynes/cm}^2$$

$$G(T_{c_2}) = 1.689 \times 10^{11} \text{dynes/cm}^2$$

$$T_{c_1} = 255°K$$

$$T_{c_2} = 300°K$$

$$\frac{\dot{\gamma}_2}{\dot{\gamma}_1} = 40$$

$2U_{k_o}$ is equal to 0.85×10^{-12} erg or 0.53 e.v.

C. Activation Volume

The most reliable verification of the Peierls process concerns agreement between theoretical and experimentally deduced activation volumes, because the activation volume by the Peierls mechanism is much smaller than that obtained for other dislocation processes. The experimental activation volumes were obtained by the effect of small changes in strain rate on the flow stress. The quantity β was defined as

$$\beta = \frac{\partial \ell n}{\partial \tau^*} = - \frac{\partial \ell n w}{\partial \tau^*} - \frac{1}{kT} \frac{\partial U_n}{\partial \tau^*} \tag{11}$$

Taking βkT as the apparent activation volume, V

$$V = \beta kT = kT \left(- \frac{\partial \ell n w}{\partial \tau^*} - \frac{\partial U_n}{\partial \tau^*} \right) . \tag{12}$$

Since the term containing w is always negligibly small, the last term of Eq. 12 is the theoretical activation volume V. Figure 20 shows the V vs τ^* curve and the low values of V in terms of b^3 agree very well with the low activation volume as predicted for the Peierls process.

Figure 21 shows the theoretical plot for the activation volume vs τ^*/τ_p for different values of α. The experimental values of $-(\tau_p/2U_k)\frac{\partial U_n}{\partial \tau}$ for different values of $\frac{\tau^*}{\tau_p^o}$, corrected for change in shear modulus with temperatures are also plotted on the same figure. Again the correlations between experiment and theory are good and the data seem to be best fitted to the curve representing $\alpha = -1$.

D. Evaluation of Line Tension of Dislocation Situated at the Peierls Valley

Dorn and Rajnak have shown that the theoretical relationship between $\frac{2U_k \pi}{a \Gamma_o} = \left\{\frac{\tau_p ab}{\pi \Gamma_o}\right\}^{1/2} \frac{.445}{1.3 \times 10^{-2\ 1/2}}$. Using the experimentally determined values of τ_p and $2U_k$ in this equation, one gets the value $\Gamma_o = 4.843 \times 10^{-4}$ dynes which is about 3 times larger than the approximated theoretical value for the line tension of an edge dislocation taken as $\frac{Gb^2}{2(1-U)}$. This minor discrepancy might be due to the presence of short range ordering in the material.

10.8 at.% Li

Instead of discussing individually the various mechanisms that might be rate-controlling for this composition, we will proceed to show how the experimental results can be correlated with the theoretical deductions of the recent approach to the Peierls mechanism discussed in the previous section. It could be shown in the same manner as in the study of 12.5 at.% Li that other mechanisms namely intersection and cross-slip are ruled out as the rate controlling mechanism.

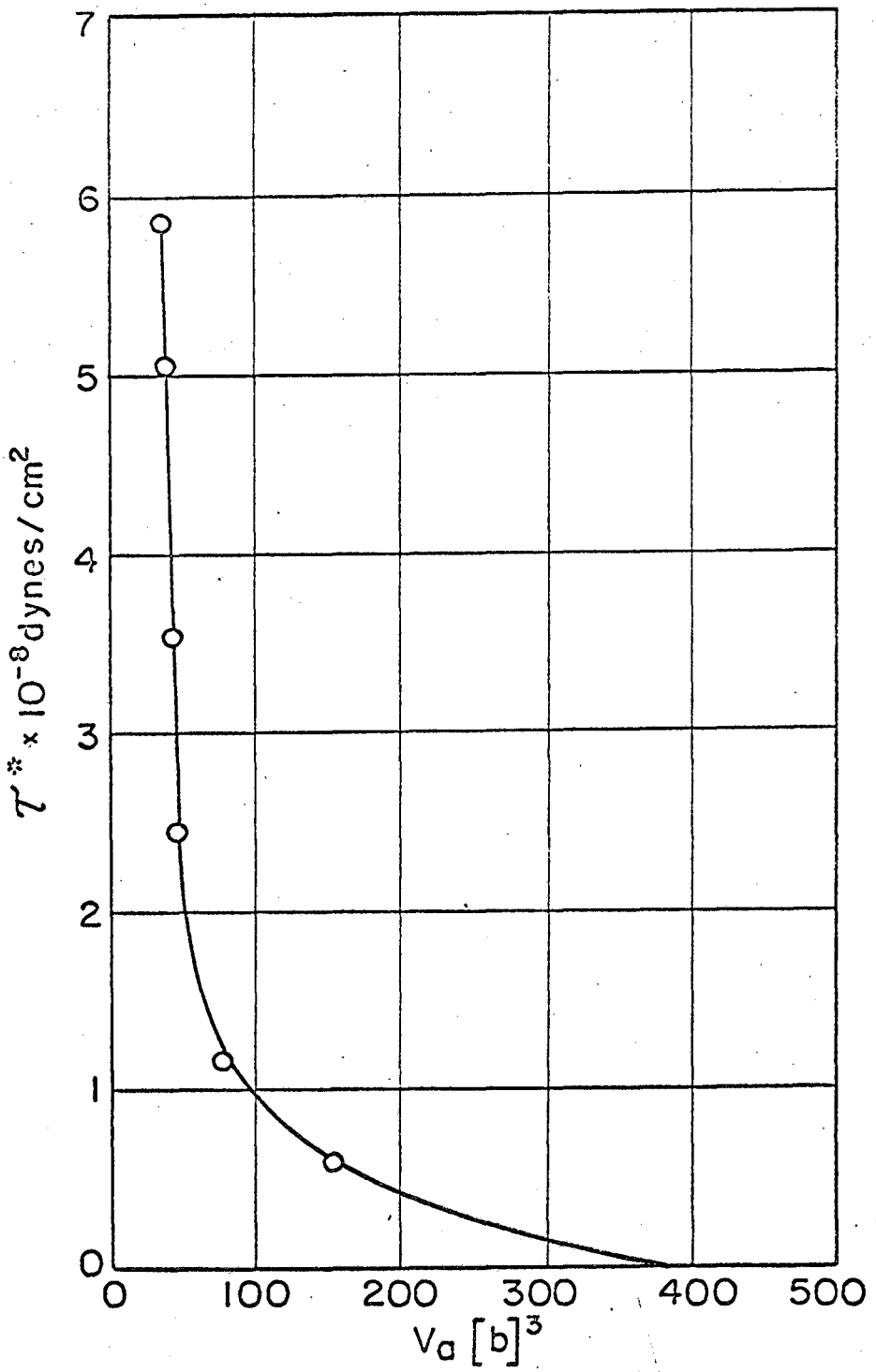

FIG. 20 THERMALLY ACTIVATED COMPONENT OF FLOW STRESS vs. APPARENT ACTIVATION VOLUME IN TERMS OF (b^3) FOR 12.5AT.% Li-Mg.

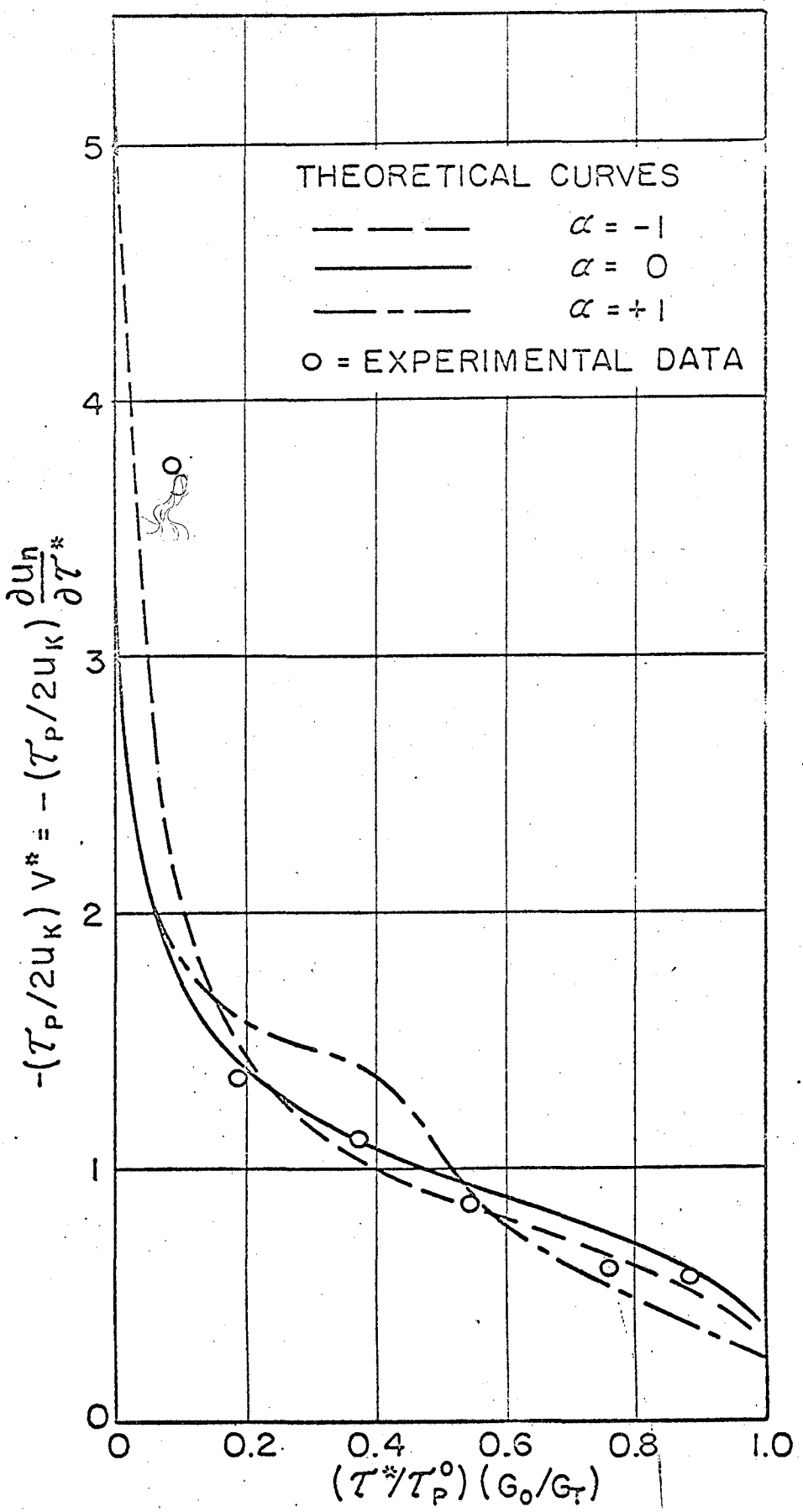

FIG. 21 THERMALLY ACTIVATED COMPONENT OF FLOW STRESS vs. ACTIVATION VOLUME IN DIMENSIONLESS UNITS FOR 12.5 AT. % Li-Mg.

E. Effect of Temperature and Strain-Rate on Critical Shear Stress

By conducting a series of preliminary tests, it was revealed that this alloy has an athermal region between about 320-360°K for $\dot{\gamma} = 1.66 \times 10^{-4}$/sec as shown in Fig. 8. Establishing this fact, temperatures of 300 and 325°K were used as reference temperatures for the determination of $\tau^* = \tau_T - \tau_{ref.} \frac{G_T}{G_{ref}}$ at two strain rates $\dot{\gamma} = 4.16 \times 10^{-6}$/sec and 1.66×10^{-4}/sec, respectively. The values of τ^* now corrected for change in shear modulus with temperature are plotted vs temperature in Fig. 22. In Fig. 22, the shape of the τ^* vs T curves agree well with those predicted by Dorn and Rajnak when plastic deformation arises from the nucleation of pairs of kinks revealing that the τ^* vs T curves have a finite slope as τ^* approaches zero.

The variation of $\frac{U_n}{2U_k}$ with τ^*/τ_p is shown in Fig. 23. The expected theoretical trends as shown by the solid curves in Fig. 23 are in excellent agreement with the experimental data and it appears again to agree best with the curve representing $\alpha = -1$.

F. Activation Energy for Nucleation of Pairs of Kinks

Using Eq. 7 and

$$K = 1.38 \times 10^{-16} \text{ergs/degree}$$

$$G(O) = 1.855 \times 10^{11} \text{dynes/cm}^2$$

$$G(T_{c_1}) = 1.705 \times 10^{11} \text{dynes/cm}^2$$

$$G(T_{c_2}) = 1.670 \times 10^{11} \text{dynes/cm}^2$$

$$T_{c_1} = 275$$

$$T_{c_2} = 325$$

$$\ln \frac{\dot{\gamma}_2}{\dot{\gamma}_1} = \ln 40$$

we get $2U_{k_o} = .89 \times 10^{-12}$ergs or .55 e.v.

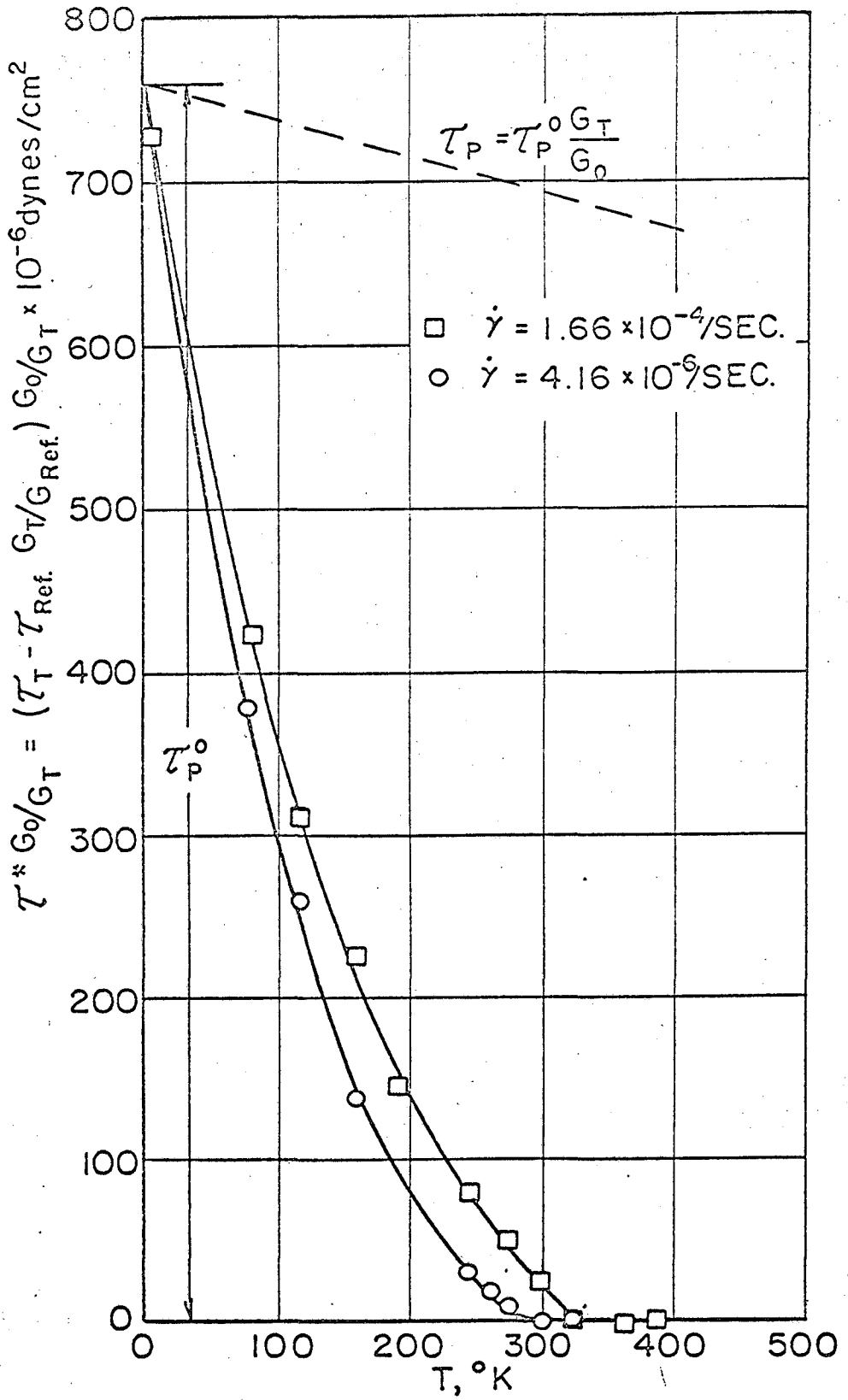

FIG. 22 THERMALLY ACTIVATED COMPONENT OF FLOW STRESS τ^* vs. TEMPERATURE FOR 10.8 AT. % Li-Mg.

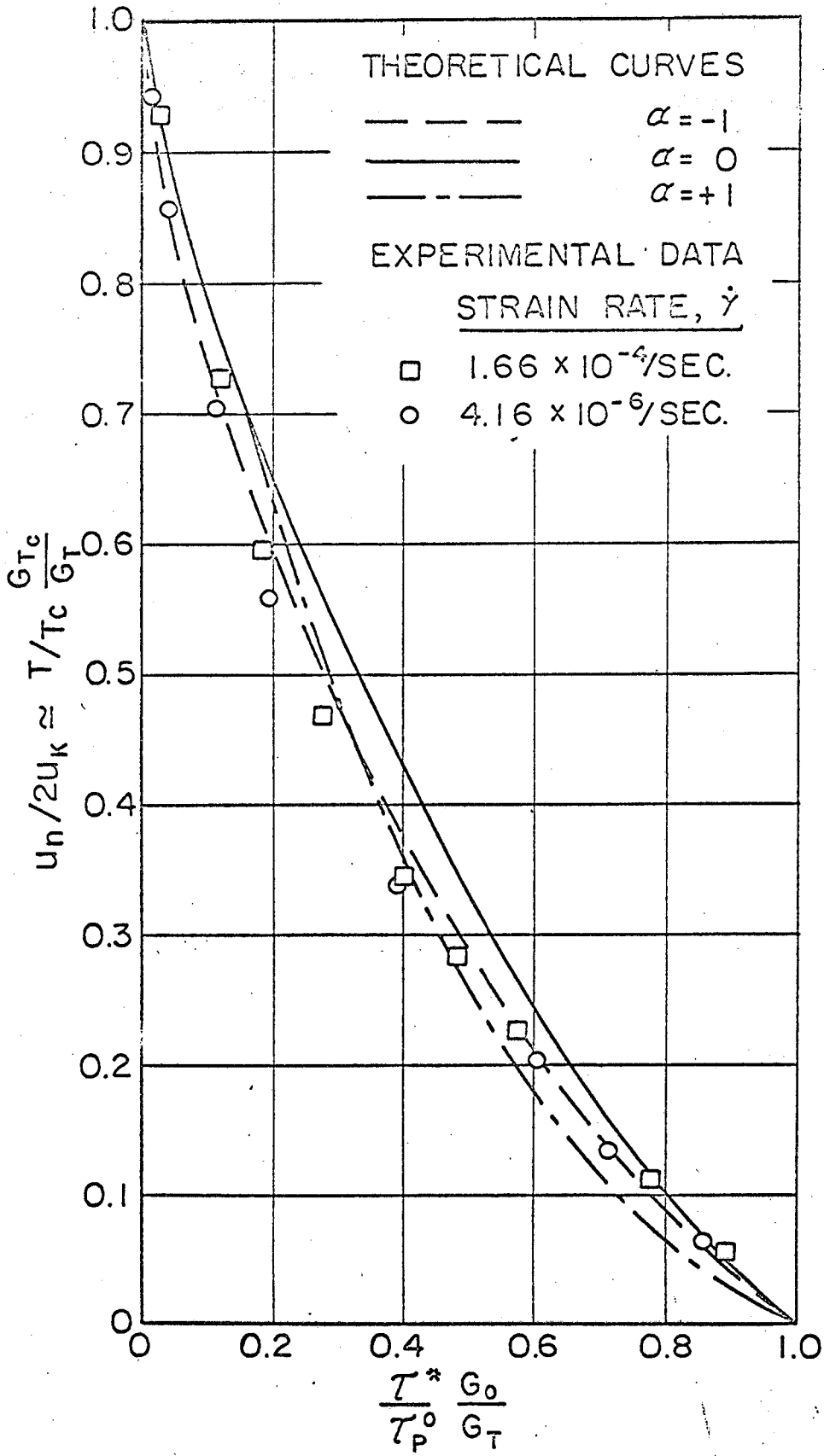

TEMPERATURE vs. THERMALLY ACTIVATED FLOW STRESS IN DIMENSIONLESS UNITS FOR 10.8 AT.% Li-Mg.

FIG. 23

G. Activation Volume

Figure 24 shows the V vs τ^* curve and the low values of V in terms of b^3 agree very well with the low activation volume as predicted for the Peierls' process.

Figure 25 shows the theoretical plot for the activation volume vs τ^*/τ_p for different values of α. The experimental values of $-\left(\frac{\tau_p}{2U_k}\right)\frac{\partial U_n}{\partial \tau}$ for different values of τ^*/τ_p°, corrected for change in shear modulus with temperature, are also plotted on the same figure. Again the correlations between experiment and theory are good and the data seem to be best fitted to the curve representing $\alpha = -1$ as was the case in the 12.5 at.% alloy data.

H. Evaluation of Line Tension of Dislocation Situated at the Peierls Valley

Using the relationship $\frac{2U_k \pi}{a\Gamma_o} = \left\{\frac{\tau_p ab}{\pi \Gamma_o}\right\}^{1/2} \frac{.445}{1.30 \times 10^{-2\ 1/2}}$ given by Dorn and Rajnak and the experimentally determined values of τ_p and $2U_k$, we get the value of $\Gamma_o = 4.742 \times 10^{-4}$ dynes which is about 3% smaller than the calculated value for Γ_o in the 12.5 at.% Li alloy.

6.8 at.% Li

The plots of activation volume vs temperature and critical resolved shear stress-temperature were shown in Figs. 14, 12, respectively, where the data reveal that there are at least two transitions taking place regarding the rate controlling mechanism in temperature range of 200-700°K. No attempt has been made to identify the mechanism governing the deformation in 350-500°K region and it is believed to be a complex of mechanisms. The region 200-350°K resembles the low temperature regions of the other two alloys where Peierls process was the rate controlling mechanism. Activation volume has a very small

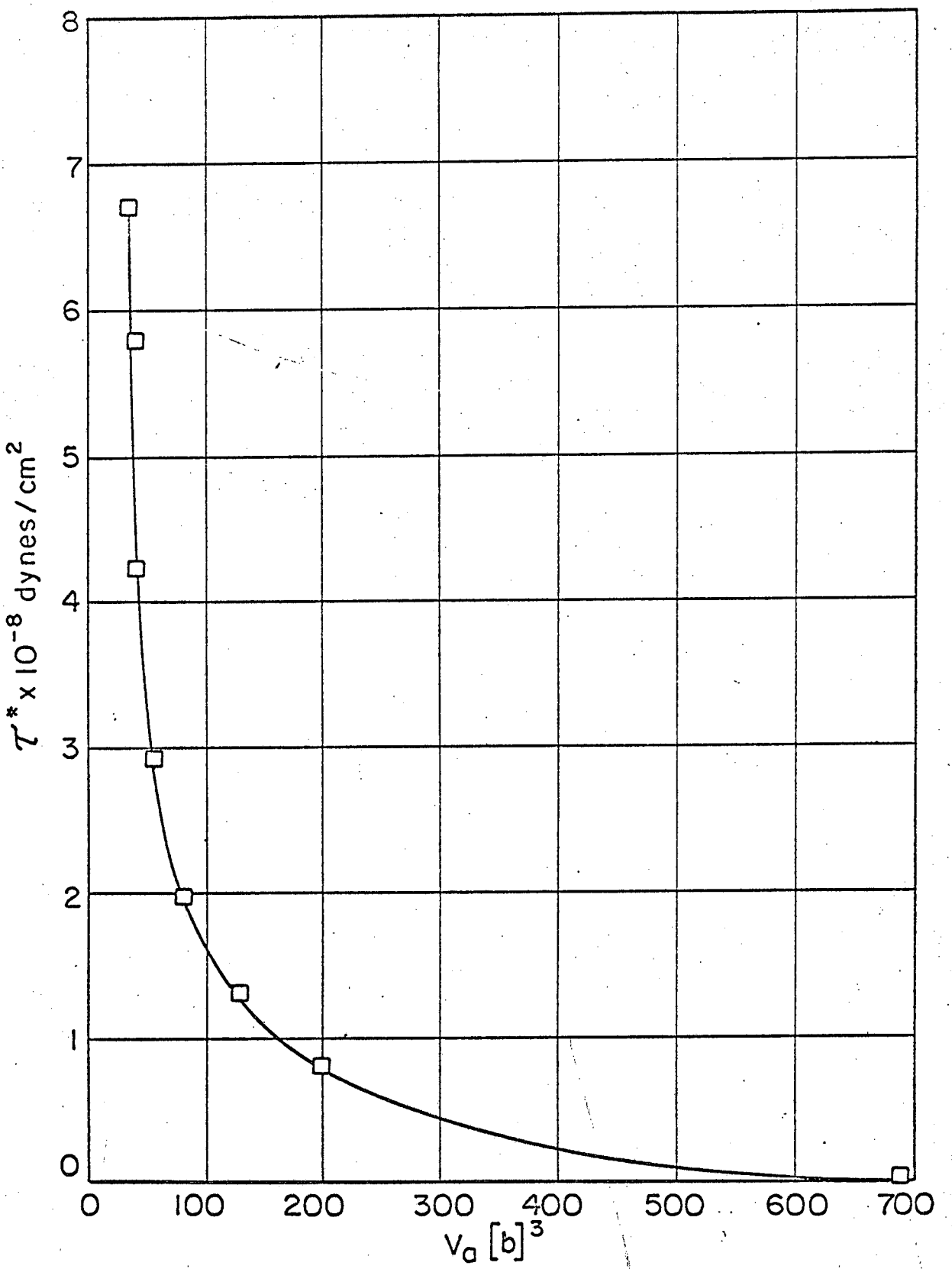

FIG. 24 THERMALLY ACTIVATED COMPONENT OF FLOW STRESS vs. APPARENT ACTIVATION VOLUME, "βKT", IN TERMS OF (b^3) FOR 10.8 AT. % Li-Mg.

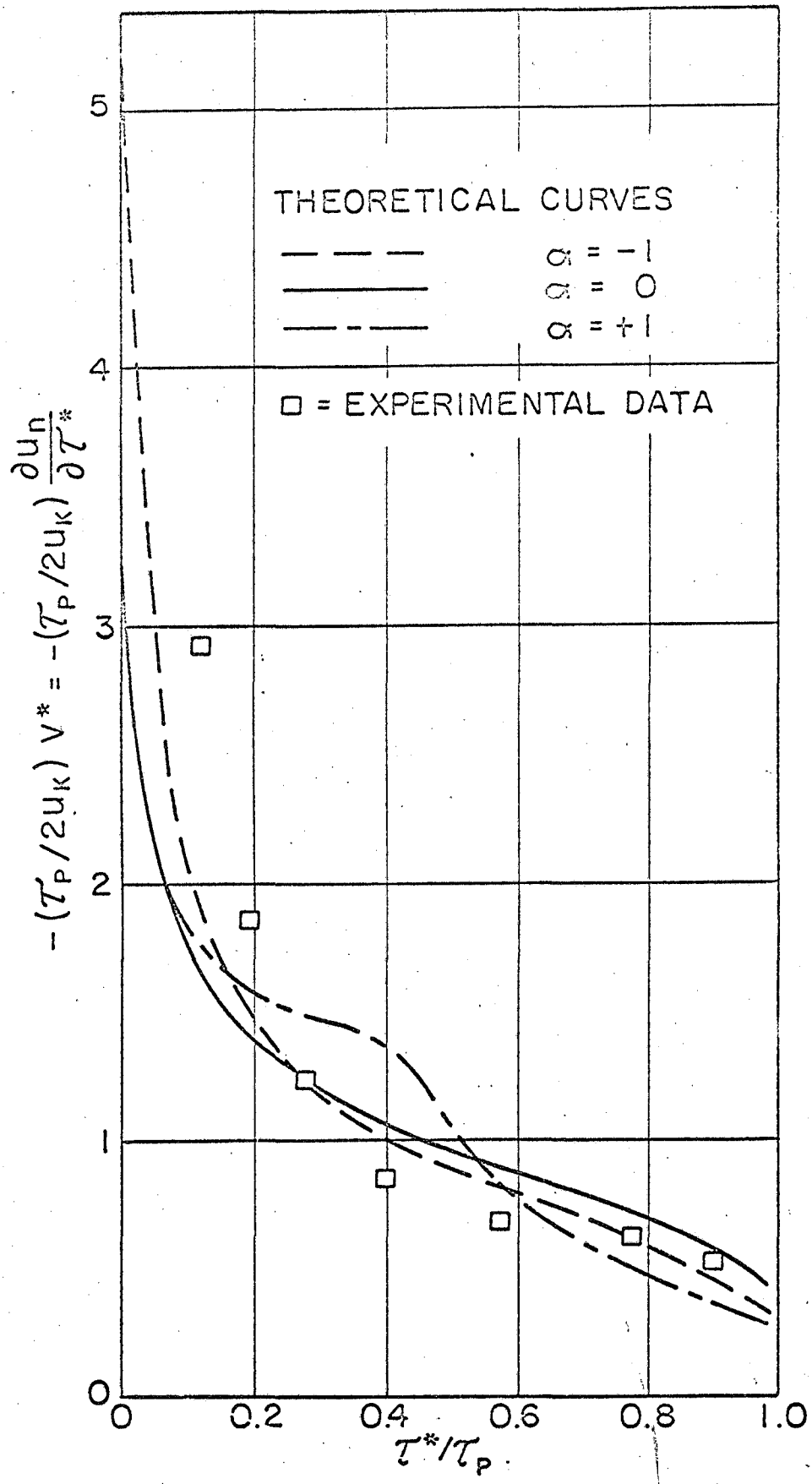

FIG. 25 ACTIVATION VOLUME vs. THERMALLY ACTIVATED COMPONENT OF FLOW STRESS IN DIMENSIONLESS UNITS — 10.8 AT.% Li-Mg.

value in this region and has the same magnitude as the activation volumes of the other two alloys at this low temperature range. The precipitous decrease in τ_c with the increase of temperature in this region also suggests that Peierls process is the rate controlling mechanism.

It will now be shown that the experimental results obtained from the third stage, i.e. at temperatures higher than about 500°K agree well with the prediction based on Friedel's theory for prismatic slip and that neither the Peierls nor the intersection mechanism can be operative as the rate controlling factor at this temperature range.

The temperature dependence of the flow stress and the magnitude of the apparent activation volume clearly deviate from those by the Peierls process.

It can also be shown that the Basinski's modification of the Seeger theory for intersection of dislocations is also ruled out. Using $\beta = \frac{1}{kT}\frac{\partial u_i}{\partial \tau} = \frac{x\ell b}{kT}$ and the experimental data in Fig. 26, we get $\ell b^2 < 20 \times 10^{-22} cm^3$ giving a value of $\rho = \frac{1}{\ell^2} > 2.5 \times 10^{11}$ for the density of forest dislocations which is unacceptable for an unworked crystal.

Having concluded that prismatic slip in this composition at this temperature range cannot be ascribed to either Peierls' mechanism or the intersection mechanism, it will now be shown that the experimental observations are in excellent agreement with Friedel's concept that prismatic slip rate is determined by the rate of nucleation of cross slip.[16]

I. Effect of Temperature on the Yield Strength

It was shown in the early section of this paper that the shear strain rate for prismatic slip according to Friedel can be written as:

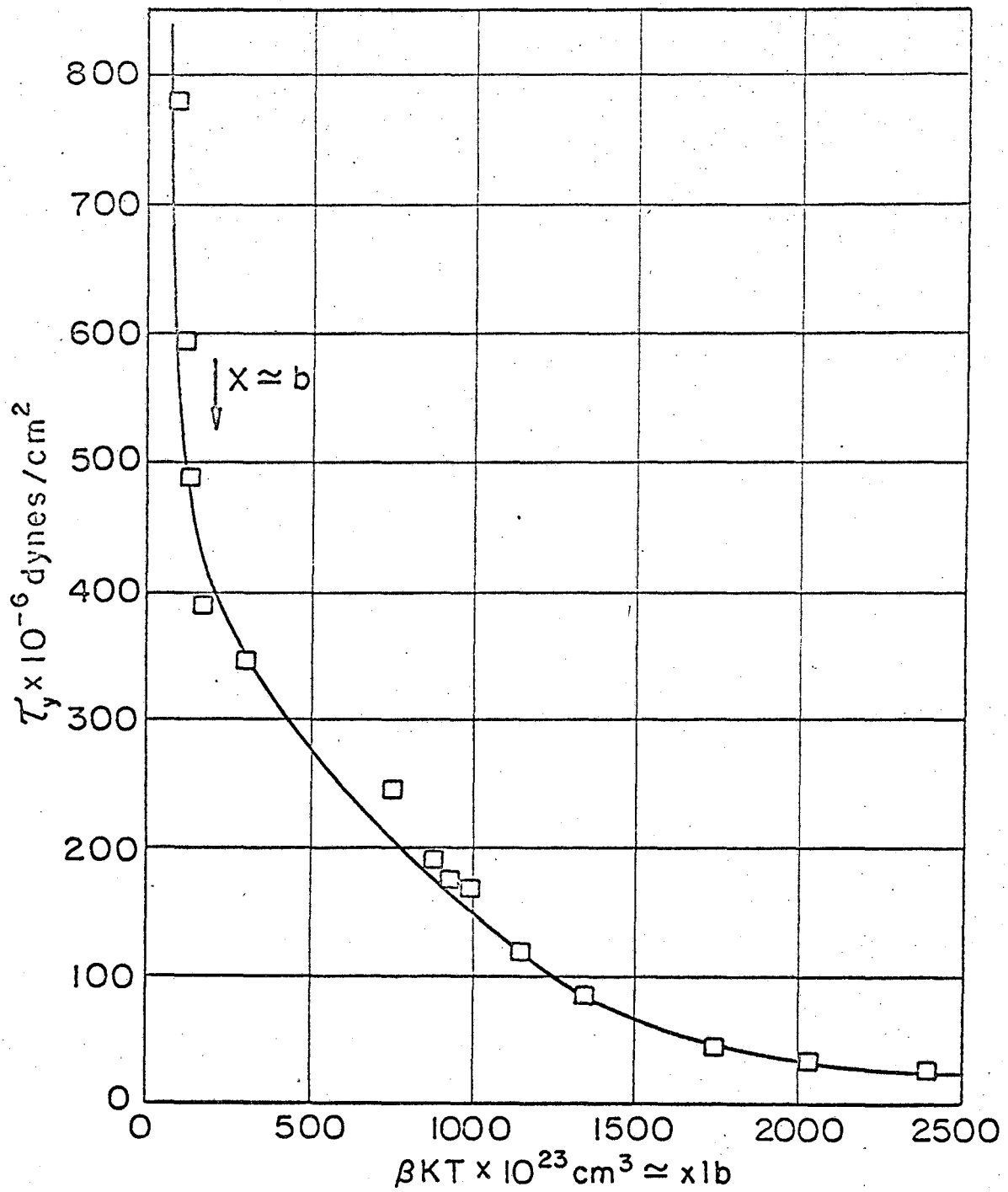

FIG. 26 CRITICAL RESOLVED SHEAR STRESS vs. "βKT" FOR 6.8 AT.% Li-Mg.

$$\frac{1}{\tau_T} = \frac{3bk}{2^{5/2}R^{3/2}\Gamma^{1/2}} \ln \frac{\lambda A b^4 \nu_o}{8R\Gamma\dot{\gamma}} + \frac{3bk\ln\tau}{2^{3/2}R^{3/2}\Gamma^{1/2}} - \frac{3bU_c}{2^{5/2}R^{3/2}\Gamma^{1/2}\,T}$$

where $\frac{1}{\tau_T}$ should decrease almost linearly with $\frac{1}{T}$. The excellent correlation of the experimental results with this prediction is shown in Fig. 27.

From the slope of the $\frac{1}{\tau_T}$ vs $\frac{1}{T}$ lines we deduce that

$$\frac{U_c}{R^{3/2}\Gamma^{1/2}} = 3.98 \text{ cm}^2/\text{dynes}. \tag{15}$$

J. Effect of Change in Strain Rate on the Stress

For Friedel's mechanism of prismatic slip

$$\beta = \left(\frac{\partial \ln}{\partial \tau}\right)_T = \frac{2}{\tau} + \frac{2^{5/2}R^{3/2}\Gamma^{1/2}}{3kT\tau^2 b} \tag{16a}$$

or

$$R^{3/2}\Gamma^{1/2} = \frac{3bkT\tau^2\beta}{2^{5/2}} - \frac{3bkT\tau}{2^{3/2}} \tag{16b}$$

Employing the values of β and τ at the yield strength for various temperatures gives the average value of

$$R^{3/2}\Gamma^{1/2} = 3.38 \times 10^{-13} \text{ ergs}^2/\text{cm}^2$$

as shown in Table IV.

Using the approximate value of $\Gamma = \frac{Gb^2}{2}$, where G is the shear modulus of elasticity (taken as 1.435×10^{11} dynes/cm^2) on slip plane, and the average value of $R^{3/2}\Gamma^{1/2} = 3.38 \times 10^{-13}$ erg^2/cm^2, we estimate $R \simeq 11.60 \times 10^{-8}$ erg/cm.

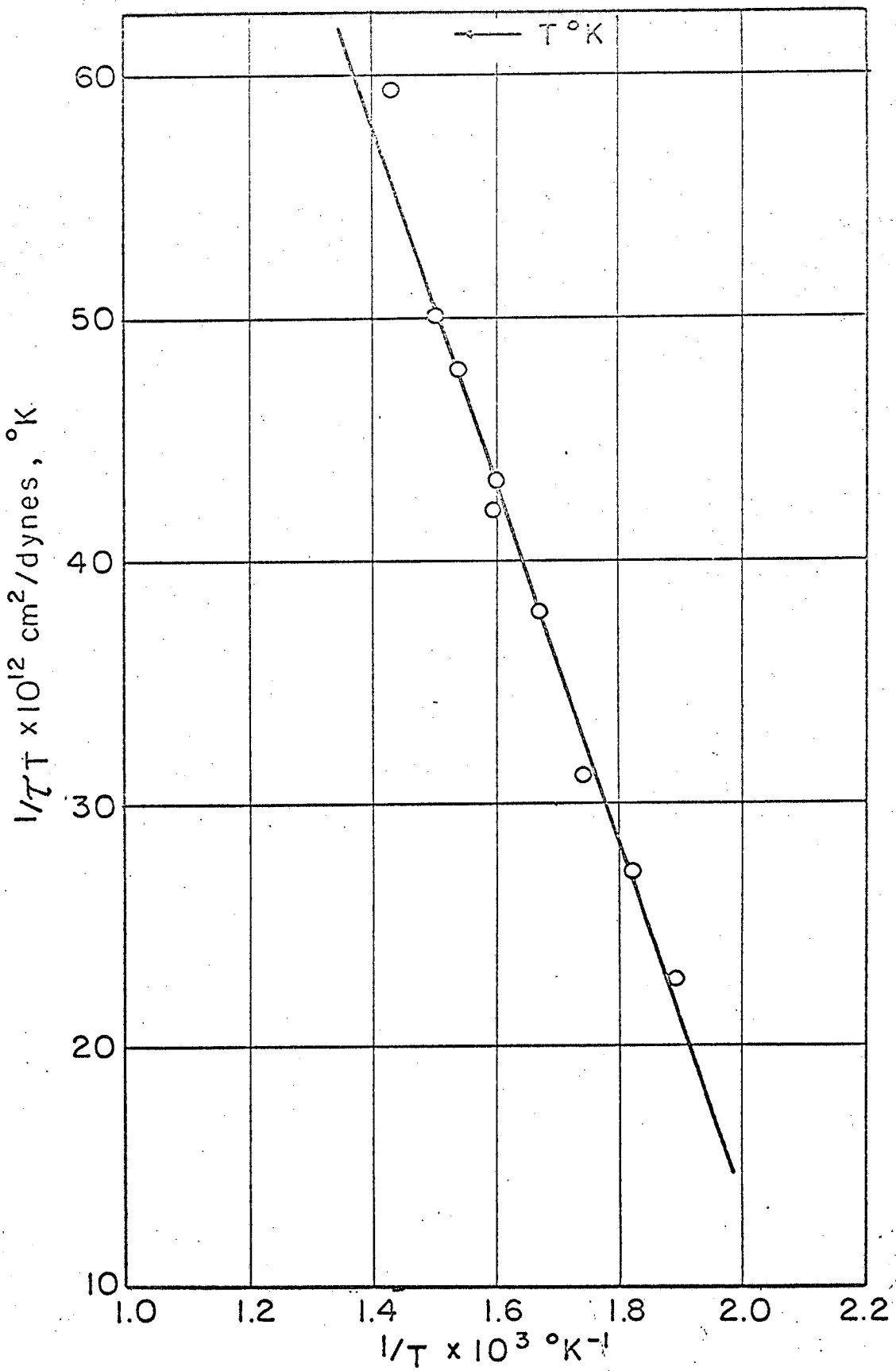

FIG. 27 THE PLOT OF $1/\tau T$ vs. $1/T$ FOR PRISMATIC SLIP IN 6.8AT.% Li-Mg.

TABLE IV

Determination of $R^{3/2}\Gamma^{1/2}$

Temperature °K	$\tau_y \times 10^{-6}$ dynes/cm^2	$\beta \times 10^8$ cm^2/dynes	$R^{3/2}\Gamma^{1/2} \times 10^{13}$ ergs^2/cm^2
600	44.1	19.4	4.1
627	37.9	21.3	3.03
650	32.7	23.4	2.8
700	26.1	35.2	3.1
714	25	36.5	3.8
		Average value: 3.38	

According to the relation[18]

$$\frac{R}{\Gamma} \simeq \frac{1}{16} \ln \frac{d}{2.7b}$$

and substituting the above values for R and Γ, the separation of the partials on the basal plane is $d \simeq 3b$.

Correspondingly upon substituting the average value of 3.38×10^{-13} erg^2/cm^2 for $R^{3/2}\Gamma^{1/2}$ in Eq. 15, U_c becomes 0.84 e.v. and according to the relation[19]

$$U_c = \frac{Gb^2 d}{30} (\ln \frac{d}{b})^{1/2}$$

the separation of the partials on the basal plane is d = 6b. The agreement between the two values for the separation of the partials "d" is considered very good in view of the theoretical approximations incorporated in the derivation of Eq. 17 and particularly 18.

The separation of dislocation partials on the basal plane of pure Mg and their constriction energy were estimated to be d = 10b and U_c = 1.54 e.v.[3] This suggests that the addition of Li decreases the separation of the partials on the basal plane and so increases the stacking fault energy.

Figure 28 which shows the temperature dependence of the critical resolved shear stress for the three alloys and pure Mg, reveals that the critical shear stress of pure Mg approaches that of 6.8 at.% Li at high temperatures where the rate controlling mechanism is cross-slipping of screw dislocations in the two materials. A comparison of the temperature sensitivity of the apparent activation volume shown in Fig. 29 also reveal that the activation volume of the 6.8 at.% Li alloy changes parallel

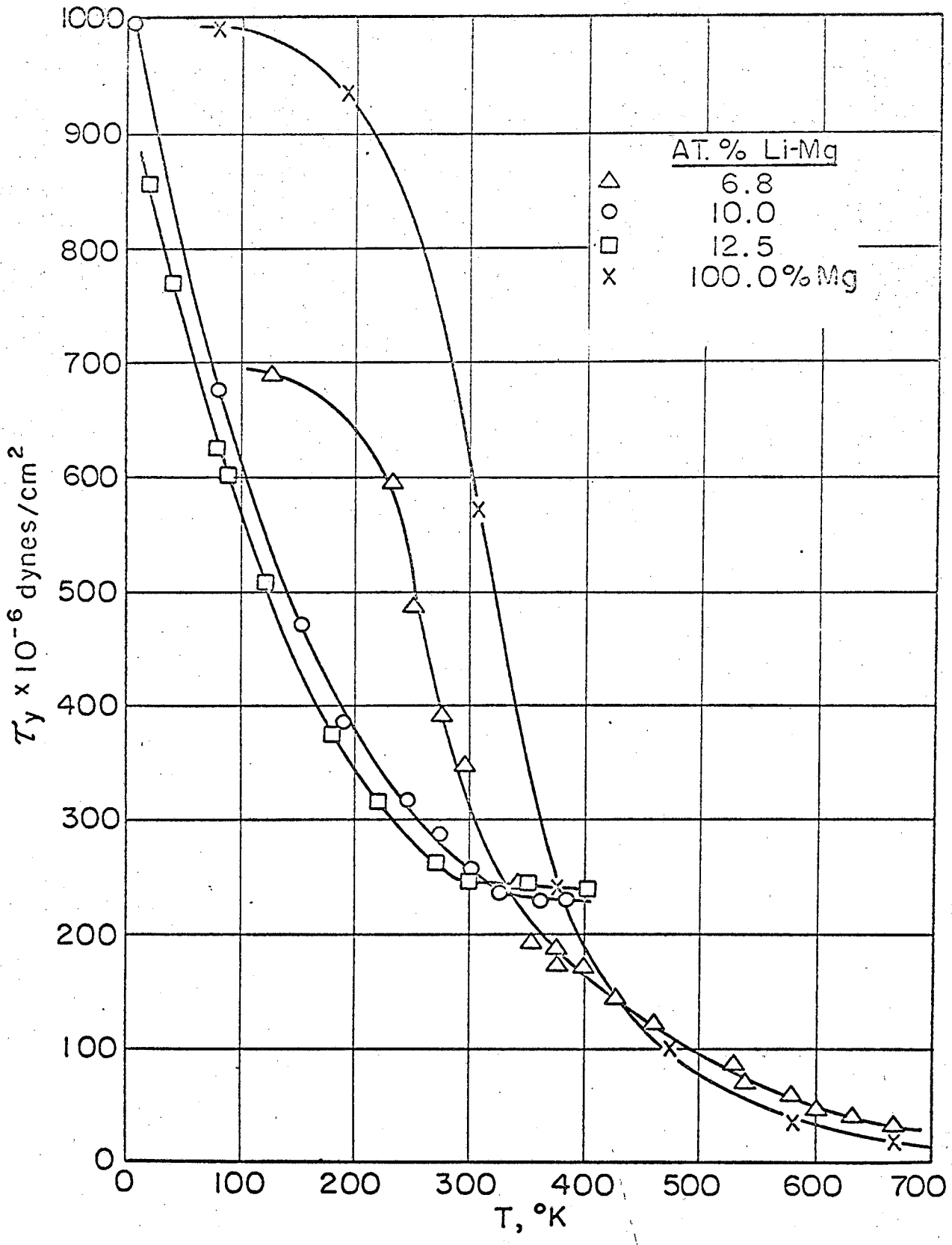

FIG. 28 CRITICAL RESOLVED SHEAR STRESS vs. TEMPERATURE FOR PRISMATIC SLIP IN PURE Mg AND Li-Mg ALLOYS.

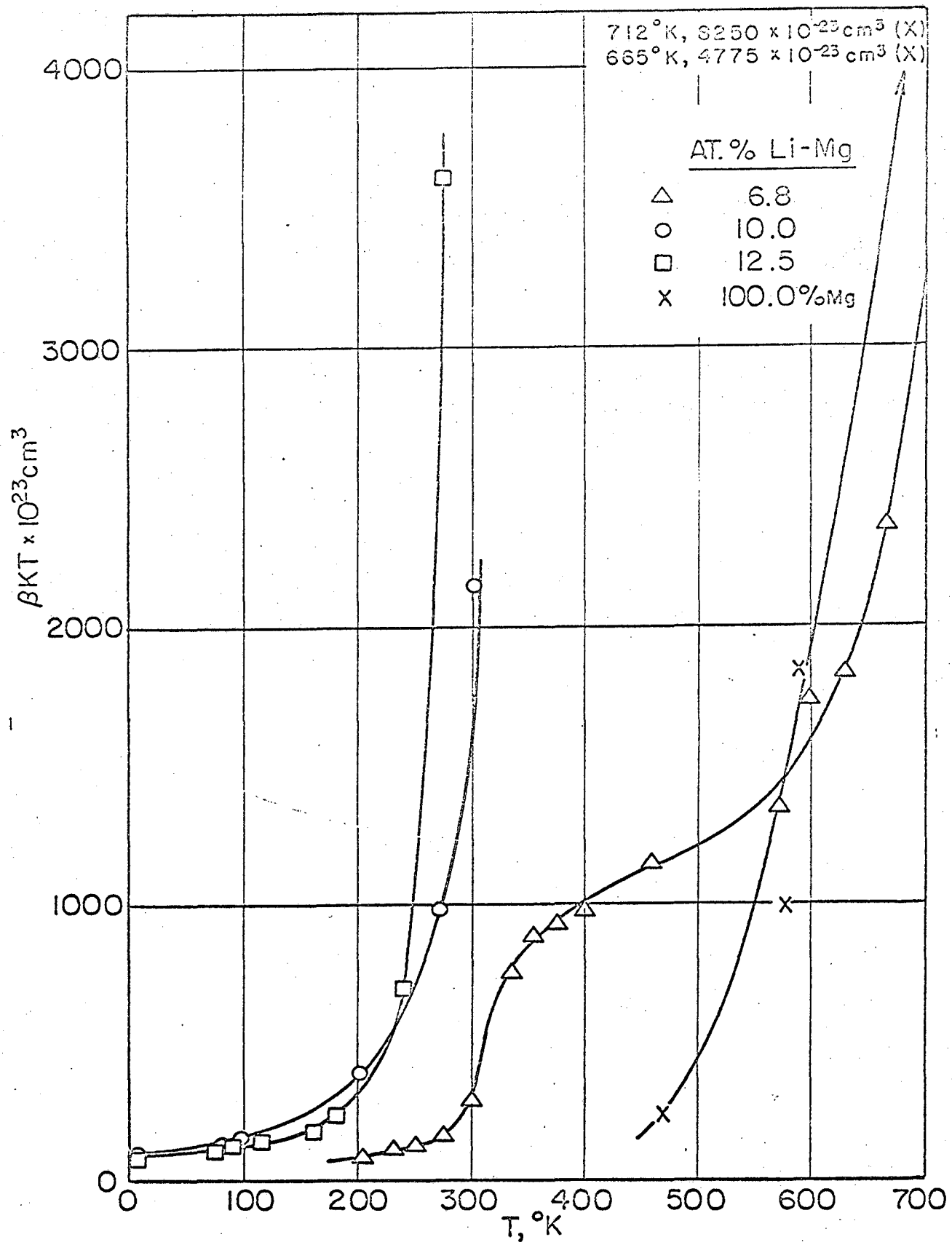

FIG. 29 ACTIVATION VOLUME, "βKT," vs. TEMPERATURE IN PURE Mg AND Li-Mg ALLOYS

to that of pure Mg at high temperature confirming that cross-slip is operative at this temperature range. The temperature dependence of the activation volume in the 6.8 at.% Li alloy is about the same as that of the other two alloys at low temperatures where Peierls process is the rate controlling mechanism. The reason for this transition from one mechanism to another with change in temperature has not been determined but it suggests that the stress required for cross-slip to take place becomes somehow less than that required for Peierls process at low temperatures.

It is also observed from Fig. 28 that the addition of Li suggests a decrease in the Peierls stress. This drop causes plastic deformation in the alloy at low temperature where there was no deformation in pure Mg oriented for this same slip.[3]

V. CONCLUSIONS

1. The decrease in the transition temperature for ductile to brittle fracturing and the drop in Peierls stress are linear with the increase in lithium content when three Mg-Li alloys containing 12.5, 10.8 and 6.8 at.% Li are studied.
2. The separation of the partial dislocations on the basal plane and their constriction energy is lowered by the addition of Li suggesting that stacking fault energy increases with lithium.
3. The relation of stress vs temperature, activation energy vs stress and activation volume vs stress obtained from the first two alloys at low temperatures agree very well with the dictates of Peierls process when the rate-controlling mechanism is the nucleation of pairs of kinks.

4. The shape of the Peierls hill for these two compositions approach a sinusoidal periodic variation with a deviation of $\alpha = -1$.
5. The activation energy of the process of the nucleation of pairs of kinks is estimated to be 0.53 and 0.55 e.v. for 12.5 and 10.8 at.% Li, respectively.
6. The apparent activation volume over the range where Peierls process is operative is approximately 30 to 50 b^3 in both these alloys.
7. The magnitude of the apparent activation volume and the relation of stress vs temperature in the 6.8 at.% Li is very much similar to those of the other two alloys at low temperatures suggesting that Peierls process is the rate controlling mechanism in the temperature range of 200-300°K.
8. Above about 500°K, the rate of prismatic slip in the 6.8 at.% Li alloy is in excellent agreement with the theory of thermally activated cross-slipping of screw dislocation extended in the basal plane.

ACKNOWLEDGMENTS

This research was conducted as part of the Inorganic Materials Research Division of the Lawrence Radiation Laboratory of the University of California, Berkeley. The author wishes to express his deepest gratitude and appreciation to Professor John E. Dorn for his excellent guidance and understanding. Thanks are also due Mr. J. Mitchell for his helpful suggestions and to Mr. E. Garlinger for preparing some of the single crystals. The author also thanks Mrs. J. Purcell for the typing of this manuscript and Mrs. G. Pelatowski for preparing the figures.

This work was done under the auspices of the U.S. Atomic Energy Commission.

REFERENCES

1. F. E. Hauser, P. R. Landon, and J. E. Dorn, "Fracture of Magnesium Alloys at Low Temperatures," Trans. AIME 206, 589 (1956).
2. F. E. Hauser, P. R. Landon and J. E. Dorn, "Deformation and Fracture Mechanisms of Polycrystalline Magnesium at Low Temperature," Trans. ASM, 48, 986 (1956).
3. P. W. Flynn, J. D. Mote and J. E. Dorn, "On the Thermally Activated Mechanism of Prismatic Slip in Magnesium Single Crystals," Trans. AIME 221, 1148 (1961).
4. W. F. Shelly, R. R. Nash, Trans. AIME, 218, 416 (1960).
5. E. Schmid and W. Boas, Plasticity of Crystals, (Hughes, London, 1950).
6. P. W. Bakarian and C. H. Mathewson, Trans. AIME, 152, 226 (1943).
7. E. C. Burke and W. R. Hibbard, Trans. AIME, 194, 295 (1952).
8. C. S. Roberts, Magnesium and Its Alloys, (Wiley, New York, 1960).
9. R. E. Reed-Hill and W. D. Robertson, Acta Met., 5, 717, 728 (1957).
10. H. Conrad, R. Armstrong, H. Wiedersich, G. Schoeck, Westinghouse Research Labs Scientific Paper 6-40104-PI.
11. T. A. Trozera, J. D. Mote and J. E. Dorn, "Activation Energies for Basal Slip in Magnesium Single Crystals," Trans. ASM, 53, 123 (1961).
12. F. E. Hauser, P. R. Landon, J. E. Dorn, "Deformation and Fracture of Alpha Solid Solutions of Lithium in Magnesium," Trans. ASM, 50, 856 (1958).
13. R. M. Quimby, J. D. Mote and J. E. Dorn, "Yield Point Phenomena in Magnesium-Lithium Single Crystals," Trans. ASM, 55, 149 (1962).

14. J. C. Fisher, Dislocations and Mechanical Properties of Crystals, (Wiley, New York, 1957), pp. 243-329.

15. Z. S. Basinski, Phil. Mag. 4, 393 (1959).

16. G. M. Rassweiler and W. C. Graube, Internal Stresses and Fatigue, (Elsevier, Hamsterdam, 1959) pp. 220-262.

17. J. E. Dorn and S. Rajnak, "Nucleation of Kink Pairs and the Peierls' Mechanism of Plastic Deformation," University of California, Lawrence Radiation Laboratory, Berkeley, UCRL-10833 (1963).

18. F. R. N. Nabarro, Advances in Physics, (Interscience Publishers, 1962) p. 271.

19. A. N. Stroh, Proc. Phys. Soc., (London) B. 67, 427 (1954).

This report was prepared as an account of Government sponsored work. Neither the United States, nor the Commission, nor any person acting on behalf of the Commission:

A. Makes any warranty or representation, expressed or implied, with respect to the accuracy, completeness, or usefulness of the information contained in this report, or that the use of any information, apparatus, method, or process disclosed in this report may not infringe privately owned rights; or

B. Assumes any liabilities with respect to the use of, or for damages resulting from the use of any information, apparatus, method, or process disclosed in this report.

As used in the above, "person acting on behalf of the Commission" includes any employee or contractor of the Commission, or employee of such contractor, to the extent that such employee or contractor of the Commission, or employee of such contractor prepares, disseminates, or provides access to, any information pursuant to his employment or contract with the Commission, or his employment with such contractor.